48646

A STUDY OF QUENCH HARDENING IN PLATINUM AND GOLD

Harold Louis Gegel

TECHNICAL DOCUMENTARY REPORT NO. ASD-TDR-62-329
May 1962

Directorate of Materials and Processes
Aeronautical Systems Division
Air Force Systems Command
Wright-Patterson Air Force Base, Ohio

Project No. 7353, Task No. 735302

B

FOREWORD

ABSTRACT

The results of this program have shown that vacancy complexes form during the quenching period when the average quenching speed is less than 10^{5}°C/second. The binding energy for divacancies in gold was estimated to be approximately 0.28 ev. The influence of increased quenching speeds is to increase the temperature recovery range for isochronal recovery. Similarly, fast quenching rates caused an incubation period in the isothermal aging experiments for gold. No incubation period was observed for platinum. The incubation period is attributed to the time necessary to develop vacancy complexes which have the appropriate geometry to influence the yield strength.

The activation energy for recovery in the quench-hardened platinum was determined to be 1.43 ev, which is less than the activation energy for self-diffusion. It was observed to be approximately equal to the sum of the constriction energies for screw and edge dislocations. The activation energy for gold is greater than that for self-diffusion. Theoretically, it was observed to be equal to the activation energy for self-diffusion plus the sum of the dislocation constriction energies.

Two distinct hardening mechanisms exist for platinum and gold when the values of the activation energy for recovery are taken into account. The hardening mechanism for gold is thought to be due to the interaction of dislocations with extended sessile dislocations, and the hardening mechanism for platinum is thought to be due to the interaction of dislocations with dislocation loops. This model has been extended to other F.C.C. metals.

Some theoretical estimates of dislocation loop sizes were made for Al, Ni, Ag, Cu, Pt, and Au. The loop size should be fundamentally related to the stacking fault energy for the respective metal. Nickel, whose stacking fault energy is approximately equal to that of aluminum, was observed to have a loop size approximately equal to that for silver. This observation was explained by the fact that the stable structure for nickel at 300°K is hexagonal close-packed.

Yield points and serrated stress-strain curves were observed for gold, but they were not observed for platinum. They were attributed to the interaction of divacancies with dislocations.

PUBLICATION REVIEW

This technical documentary report has been reviewed and is approved.

B. K. MORSE
Actg Chief, Advanced Metallurgical
   Studies Branch
Metals and Ceramics Laboratory
Directorate of Materials and Processes

TABLE OF CONTENTS

LIST OF FIGURES

LIST OF FIGURES (Continued)

LIST OF TABLES

INTRODUCTION

Kauffman and Koehler (1) showed that the presence of a nonequilibrium number of vacancies quenched into metals could be detected experimentally by electrical resistivity measurements. When close-packed metals are quenched from high temperatures, the vacancy concentration at the elevated temperature is retained at room temperature or lower if the appropriate quenching rate is used. If it is assumed that the quenched-in extra resistivity is a function of the number of excess vacancies quenched into the lattice, then it may be shown that the resistivity is related to the energy of formation of a vacancy, E_f, and to the temperature by

$$\Delta f = A \exp\left(-E_f / RT\right) \tag{1}$$

The constant A is equal to the product of the increase in resistivity per unit concentration of vacancies and to the entropy of vacancy formation, exclusive of the entropy of mixing. The extra resistivity attributable to vacancies has been observed in quenched platinum (2) (3) (4), gold (1) (2) (5), aluminum (7) (8) (9), and copper (6). An excellent review article on the theory and experimental techniques is presented by Broom (10). Simmons and Balluffi (11) (12) (13) measured the equilibrium concentrations of vacancies in silver and aluminum at temperatures near their melting points, and found that the resistivity attributable to the vacancies at these high temperatures was in agreement with the concentration calculated from lattice parameter and atomic volume changes measured at these temperatures.

J. J. Jackson (14) studied the rate of production of vacancies in gold by a pulse heating technique, and concluded from energy considerations that vacancies can be produced at observed rates only at grain boundaries or dislocations. These results imply that the equilibrium concentration of vacancies could be measured by observing the change in length of a metal whisker which has a large surface to volume ratio. The extra resistivity due to vacancies produced at the grain boundary was determined to be about one-fifth of the total increase. The activation energy for the increase in extra resistivity was found to be greater than that for vacancy migration and the increase was attributed to dislocation climb. Dislocation climb at high temperatures enhanced the rate of vacancy production.

Vacancies that were created at jogs in the dislocations diffused through the lattice at high temperatures as single vacancies. The initial annealing rate was observed to be greater in the pulsed wires than in the wires quenched with the equilibrium vacancy concentration at the same temperature. This is evidence that the same dislocations act as both sources and sinks for vacancies.

The excess vacancies quenched into the metal migrate to vacancy sinks during low temperature anneals. If this migration is random with no occurrence of clustering, that is, fixed sink decay, then the quenched-in resistivity decays exponentially. (15)

$$n = n_0 \exp\left(-a\, n_s t\right) \tag{2}$$

Manuscript released by the author March 1962 for publication as an ASD Technical Documentary Report.

where n is the number of vacancies remaining after time t, n_o is the initial number present immediately following the quench, n_s is the number of available sinks, and α is a constant. Equation (2) may be rewritten in terms of τ, the half-life of vacancies.

$$\tau = \tau_0 \exp(E_m/RT) \qquad (3)$$

where τ_o is a constant and E_m is the activation energy for vacancy migration. However, it has been observed that typical first order annealing curves are obtained only when the initial vacancy concentrations are very low.

The order of the decay kinetics and the jump frequency will be reflected by the nature of the vacancy sinks, the number of sinks, and possible athermal nucleation. Fisher, Hollomon, and Turnbull (33) have developed a general theory of nucleation which can be applied to vacancy cluster nucleation which occurs during the quenching period. They emphasize that nuclei do not leap into existence by a single fluctuation, but arise from embryos that change their size continuously by losing or gaining atoms (vacancies) one at a time from the surrounding matrix. Athermal nucleation, which is very important in certain phase transformations, can be of similar importance in the decay kinetics involved in vacancy annihilation. If the temperature change is rapid enough, the initial distribution of defects will not differ too appreciably from that corresponding to the annealing temperature. Deviations from the steady state condition also will be present when the temperature change is gradual. Every reaction must begin with a transient rate of nucleation. Kimura, Maddin, and Wilsdorf (15) have suggested that more complicated decay kinetics result from changes in the sink concentration during annealing. Such sinks could possibly develop during the quenching period. "Variable-sink decay" (15); N_s; such occurs when sessile rings form on the (111) planes due to vacancy clustering. The majority of the available sinks are of the sessile dislocation type. The variable sinks obey the following relation.

$$n = n_0 (\cosh \alpha KT)^{-2} \qquad (4)$$

where K equals $\pi/2 \, (n_s n_o)^{1/2}$ and $\pi \, (N_s n_o/2)^{1/2}$ for single and divacancies respectively. and N_s is the number of sessile rings. Equations for vacancy decay involving both fixed and variable sinks have also been developed by Kimura, et al.

Recently there have been several important investigations in the area of point defects and the mechanical properties of pure metals. Such studies have noted an increase in the yield stress of zinc (16), aluminum (17) (18), gold (19) (20), and copper (21). The observed yield strength increases of 200 and 500% after quenching and aging have been attributed to the formation of stable hardening configurations resulting from the annihilation of quenched-in vacancies and divacancies. The nature of the slip lines developed by the tensile test indicate that stacking faults are important defects formed by clustered vacancies.

Stacking faults in quenched samples are important in the hardening of latent slip planes, which apparently occur in the quenched and aged face-centered cubic metals, since little evidence exists for strain hardening or lattice distortion in these metals. Research on alpha brass by Maddin, Mathewson,and Hibbard (34) shows that strain hardening and lattice distortion (as shown by X-rays) are absent when slip is confined to a single set of parallel slip planes, or to two nonparallel sets of planes that use a common slip direction; whereas both strain hardening and distortion become marked as soon as slip

commences on planes having a different slip direction. The inherent stacking fault energy of a metal may be one of the important factors in determining the vacancy annihilation mechanism.

Kuhlmann-Wilsdorf (35) has pointed out that if vacancies coalesce to form plate-shaped regions on the closest-packed planes, they finally give rise to dislocation rings. When the dislocation has a Burgers vector equal to $1/3[111]$ the dislocation ring marks the perimeter of a stacking fault. The magnitude of the stacking fault energy will determine the stability of the configuration. Metals like aluminum and nickel, which have high attacking fault energies, will favor another more stable arrangement. Energy-wise, it may be more favorable for a dislocation ring of Burgers vector $1/6[211]$ to form and eliminate the stacking fault. The latter can then react with the original dislocation line to form a so-called "R-dislocation" with the Burgers vector $1/2[011]$.

The present research extends the knowledge of quench hardening in face-centered cubic metals by systematically investigating the change in yield strength of platinum and gold after quenching from temperatures near their melting points and aging at various temperatures. These experiments should yield information relative to vacancy clustering and vacancy decay mechanisms, and they should also provide information which can be used to determine the mechanism of hardening.

In this investigation, wires of pure platinum and gold were heated to 1500° and 1000°C respectively where vacancies are abundant; held for sufficient time to reach an equilibrium temperature, and then quenched. Several extreme quenching rates were used on the gold specimens to determine the influence of quenching rate on the annealing characteristics and to investigate the possibility of athermal nucleation. Platinum and gold were studied, since information concerning the electrical resistivity behavior of both metals was available; and since neither metal forms an oxide which is stable at high temperatures.

<center>EXPERIMENTAL PROCEDURE</center>

Platinum wire specimens, 99.999% pure and 0.010 inch diameter, were heated by passing a current through them. The temperature of the wire was calculated from electrical resistance measurements to an accuracy of ±15°C. The resistivity of platinum as a function of temperature is given in figure 1. The specimens were heated in air, and the radial heat loss was found to be much greater than the heat flux conducted along the wire. Only specimens that were uniform along a nine-inch gage length could be used. Cooling by conduction down the 0.002 inch potential leads was negligible.

The quenching rate was measured by a resistivity technique, that is, the potential leads were connected to a voltage limiter and in turn connected to the vertical input of a Hickok Oscilloscope. Upon decreasing the heating current through the hot specimen to a low value, the scope trace was effectively a plot of specimen temperature versus time. The specimens experienced a quench rate of 37,500°C/sec when lowered into a water bath maintained at 23°C. A mercury switch fixed to a movable arm cut off the heating current in the wire upon contact with the water. Trial quenching procedures prior to actual operation allowed accurate positioning of this switch. All specimens were cooled at approximately the same rate by this technique. A typical temperature versus time curve appears in figure 2. Prior to heating to the quenching temperature, each specimen was heated to 1650°C for two minutes and then slowly cooled to room temperature. This preheat treatment was introduced to standardize the grain size for each specimen and to produce a

dislocation structure which was relatively the same in each specimen. A schematic diagram of the heating and quenching circuit is shown in figure 3.

Annealing studies were carried out on quenched specimens by transferring them to a salt or lead pot depending on the aging temperature. The specimens were protected from the environment by a small quartz tube. The lead and salt pots were used for aging times of less than forty minutes, and a resistance wound furnace was used for the longer aging times. The temperature was controlled to within ±1°C. An air-cool to room temperature followed the aging of the specimens.

The aging temperatures selected were 300°, 400°, 500°, and 600°C. The isochronal electrical resistivity curve shows that this range of temperatures covers the recovery range for quenched platinum. Piercy's (27) isochronal resistivity curve is presented in figure 4.

The quenching technique was altered slightly for the gold wires. The gage length of the wire was decreased to four inches to reduce the amount of sag in the wire at 1000°C. The ends of the gold wire were attached to a 0.030 inch nichrome wire. When the heating current was applied to the gold specimen the nichrome wire in contact with the gold wire heated to a red glow for a distance of about one-quarter inch. This technique prevented the loss of heat down the grips which had proved to be somewhat of a problem. The gold specimens were quenched into three different quenching mediums.

Water, dibutyl pthalate, and mineral oil were used as the quenching baths for the gold specimens. The purpose of using the different quenching mediums was to obtain three different quenching rates which differed from each other by at least one order of magnitude. The quenching rates obtained respectively were 10^7, 10^5, and 10^4°C/sec. Figure 5 gives a picture of the different cooling curves.

Gold specimens were quenched from 1000°C, using the three different rates of quenching, and subsequently aged for ten minutes over a temperature range from room temperature to 500°C. This type of aging experiment is termed isochronal aging, and its purpose is to determine the temperature recovery range for a given quenching rate. Isothermal aging experiments were also made, and the aging temperatures were 100° and 200°C. Immediately after quenching each specimen was placed in the aging furnace or oil bath. The transfer time from the quenching apparatus to the aging furnace or oil bath was observed to be about two minutes. After the specimens were aged for the appropriate amount of time, they were stored in liquid nitrogen until they were tensile tested. The time to mount each specimen in the tensile fixture was about one minute. The handling time apparently did not have any deleterious effects on the property changes recorded.

The tensile tests of both the platinum and gold specimens were performed on an Instron Tensile Machine. A B load cell was used which provided adequate sensitivity up to and including fracture of the wires. The 0-500 gram scale was used to test the platinum specimens, and the 0-200 gram scale was used for the gold--up to the yield strength. The range scale was subsequently switched to the 0-500 gram scale beyond the offset yield strength.

Specifically designed grips were used to hold the wire specimens in the tensile machine. The lower grip holder was designed to permit the movement of the grip in the horizontal plane to center the grip. A sketch of the grip holder appears in figure 6. The grips can be easily adapted to hold wires of different diameters by changing the radius of the grips to that of the new wire diameter. The grips are shown in figure 7.

The difficulty of the wires breaking in or at the grips caused some concern when preliminary tensile tests were performed. This problem was overcome by spraying the ends of the wires, which are placed in the grips, with clear Acrylic plastic spray. Each tensile specimen was coated with a thin layer of the plastic spray over the area which was placed in the grips. The overall length of the tensile specimen was three inches, and the gage length used was one inch. The other two inches were in the grips. All fractures occurred within the inch-test length, and usually near the center of the specimen.

IMPURITIES IN PLATINUM AND GOLD

TABLE 1

SPECTROGRAPHIC ANALYSIS FOR IMPURITIES IN
PLATINUM AND GOLD

1. Platinum				
Palladium		2 ppm	Magnesium	less than	1 ppm
Calcium		1 ppm	Silicon	less than	1 ppm
Copper	less than	1 ppm	Silver	less than	1 ppm
Iron		1 ppm	Sodium		1 ppm

2. Gold				
Palladium		3 ppm	Magnesium		3 ppm
Rhodium	less than	1 ppm	Calcium		2 ppm
Silver		26 ppm	Silicon		12 ppm
Copper		1 ppm	Lead	less than	1 ppm
Iron		1 ppm	Aluminum		4 ppm

RESULTS AND OBSERVATIONS

A. Platinum

1. Aging Curves

The shape of the aging curves indicates that the aging phenomena of the quenched specimens are very complex. This is shown in figure 8 and figure 9. Immediately after immersion in the aging bath, the yield strength increased suddenly, which was subsequently followed by several maxima and minima in the curve before a gradual increase to the saturation strength of the aged material was reached. After the saturation strength was reached, overaging began to occur. A similar behavior was observed for copper (21). The time to reach one-half the saturation strength, τ 1/2, for the aging temperatures of 300°, 400°, 500°, and 600°C was approximately 100, 13.2, 2.7, and 1.2 minutes respectively. Because of the complex form of the aging curves, it is difficult to estimate the time to reach one-half of the saturation strength. The time to reach the saturation strength of the material, τm, for aging temperatures of 400°, 500°, and 600°C was approximately 1300,.68, and 6.4 minutes respectively. Because of the aging time for the 300°C anneal ran for a maximum time of only 60,000 minutes, a time could not be estimated accurately. However, extrapolation of the log time to reach saturation strength against $1/T_a$, the

reciprocal of the absolute aging temperature, gives a value of 86,000 minutes for an aging temperature of 300°C.

2. Activation Energy

The activation energy for the hardening process was determined by plotting log time from the aging curves against $1/T_a$. The activation energy resulting from the plot of log τ1/2 against $1/T_a$ was found to be 0.69 ev, and the activation energy determined by using the time to reach the saturation strength was found to be 1.43 ev. Plots of these points are given in figure 10 and figure 11. The initial hardening peak, which is shown in figure 8, was investigated by computing the activation energy for four different stress levels. These stress levels were 3.6, 4.0, 4.2, and 4.3 Kg/mm^2 and the corresponding activation energies were 1.19, 1.28, 1.33, and 1.05 ev respectively. These plots are shown in figure 12. These various activation energies indicate that there is no unique process for the annihilation of vacancies which would be characterized by a single activation energy. Table 2 gives a list of activation energies taken from the literature for various vacancy annihilation processes in platinum.

3. Metallography of Deformed Wires

Examination of the wires optically showed that slip occurred along the primary slip system and that conjugate slip eventually takes over. Double slip involving primary and conjugate slip occurred only in the region near the fracture. The slip lines near the fractures are coarse and wavy, while the slip lines away from the fracture are long, sharp, and straight with some cross slip in evidence. The nature of the slip lines in shown in figures 13 through 20. The appearance of the slip lines indicates a non-turbulent deformation process which is indicative of a low rate of work hardening. Figure 21 illustrates a typical load-elongation curve for the platinum wires which shows a low degree of work hardening. The recrystallization texture was determined after the wires had been heated to 1650°C, and it was found to be [$\bar{1}$00].

4. Load-Deformation Curves

The load-elongation curves for the quenched and aged samples show little evidence of work hardening. An example of a typical load-elongation diagram is given in figure 21. This curve has a characteristic drop in the load which occurs after an appreciable amount of deformation has taken place. Throughout the length of the specimen there was little evidence of necking which is an indication that conjugate slip was occurring. The yield strength at 0.2% offset of the quenched and aged specimens at the saturation strength was greater than the as-quenched value by about a factor of 2. Maddin and Cottrell (22) observed that the behavior of quenched and aged aluminum single crystals exhibited a high yield strength and a low work hardening coefficient. This behavior is possibly related to latent hardening of the conjugate slip systems. Metallographic examination of the wires showed them to have a bamboo structure which consists of a series of single crystals. This type of structure can account for the shape of the load deformation curve. The fact that a bamboo structure is present suggests that the lattice of one or several grains did not rotate into another symmetry triangle. However, a close look at the characteristics of the slip lines reveals that they cross the grain boundaries without changing direction markedly in the new grain. It appears that each grain has very nearly the same orientation.

TABLE 2

ACTIVATION ENERGIES FOR RECOVERY PROCESSES IN PLATINUM

Method of Introducing Defects	Recovery Temp. Range °C	Activation Energy ev	Reference
Extended at -196°C	-150 to -170 -10 to 70	0.22 0.99	Manintveld (1954)
Extended at 20°C	70 to 100	1.19	Dugdale (1952)
Extended at -196°C	0 to 100 200 to 4400	 0.73	 Piercy (1960)
Quenching from above 1600°C	- - - - - - -	1.1	Lazarev and Ovcharenko (1955)
	300 to 500	1.10	Bradshaw and Pearson (1956)
	300 to 500	1.13	Piercy (1960)
Quenching from 1100 to 1500°C	450 to 580 450 to 580 300 to 600	1.42 1.48 1.43	Ascoli (1958) Bacchella (1959) Present Work*
Reactor Irradiation at 50°C	70 to 90 100 to 300	1.19 1.43	Dugdale (1952 Piercy (1960)

*Referenced workers used the change in resistivity technique to follow the aging process while this work involved the change in yield strength method.

B. Gold

1. Aging Curves

Initially the response of the gold wires to heat-treatment caused some concern, since there was no immediate change in the yield strength as was anticipated from results reported in the literature. Meshii and Kauffman (36) reported that gold specimens aged at 100°C at a rate of 30,000°C/sec produced maximum saturated hardening. The initial quenching rate used in these experiments was approximately 10^7°C/sec which is three orders of magnitude greater than that commonly used by previous investigators.

In order to resolve the problem, isochronous aging experiments were made to determine the temperature recovery range, and to determine if the quenching rate influenced the recovery temperature. Three different quenching rates which differed from each other by at least one order of magnitude produced three distinct temperature recovery ranges. The temperature recovery ranges for the quenching rates of 10^7, 10^5, and 10^4°C/ sec are 300° -500°C, 150° -300°C, and room temperature to 150°C respectively. These isochronal aging results are presented in figure 22.

It should be observed that the slowest quenching rate of 10^4°C/sec would have permitted the development of the maximum saturated strength in one hour at 100°C which is in good agreement with the results reported by Meshii and Kauffman (36). The isochronal aging characteristics can be related to the number of vacancy complexes formed during the quenching period. This matter will be discussed in detail in another section.

Isothermal annealing experiments were made at 100° and 200°C with specimens quenched from 1000°C at a quenching rate of approximately 10^5°C/sec. The results of these experiments show that an incubation period exists before any appreciable change in the yield strength occurs. The duration of the incubation periods for the 200° and 100°C isothermal aging curves is approximately one hour and 16 hours respectively.

The shape of the remainder of the aging curves after the incubation period was identical to that obtained for platinum. These aging curves are presented in figures 23, 24, and 25. The gold specimens were not aged at a high enough temperature to show an overaging effect as was obtained for the platinum experiments. The maximum aging time was 1000 hours. No activation energies were calculated for the various stages of the aging process, since there were insufficient specimens available to conduct aging experiments at higher temperatures.

2. Mechanical Behavior and Slip Line Appearance

Examination of the wires optically after being plastically deformed revealed that slip occurred predominantly on the primary slip system. There was less evidence of cross-slip in the gold specimens than in the platinum specimens. This difference in the frequency of cross-slip can be explained by the relative difference in stacking fault energies of these metals at room temperature. The stacking fault energies for gold and platinum at room temperature are 17 and 35 ergs/cm^2 respectively (37).

The general shape of the stress-strain curve for gold was the same as that for the platinum wires, as they both exhibited a very low rate of work hardening. There was no attempt to carry every tensile test out to fracture, but enough tests were taken to fracture

in order that the general trend in the total elongation could be observed. The elongation was observed to decrease with increased aging time. Two specimens aged for 800 hours at 100°C exhibited a total elongation of only 1%. A decrease in the ductility is an indication that the latent slip systems were hardened by some defect, probably stacking faults. When slip is confined to a single slip system the total amount of slip that can occur on that one system is limited. The proportional limit of the stress-strain curve was observed to increase to a maximum value at the point on the aging curve where the saturated yield strength was observed to become constant. Figure 25 shows this proportional limit change. This increase in the proportional limit may be due to the critical shear stress increase on the secondary slip planes which is reflected by their latent hardening.

Yield points were observed in gold specimens which were aged for times less than six hours at 100°C. These yield points occurred without the necessity of prestraining or varying the strain rate. Figures 26 and 27 show the stress-strain curves for specimens aged for 15 minutes and six hours respectively. No yield points were observed with the platinum specimens given comparable heat treatments. It is believed that these yield points were caused by dislocation-vacancy interactions which temporarily pin the dislocations.

Figure 28 shows a stress-strain curve possessing a yield point in a specimen that had been aged for 15 minutes at 150°C and had been plastically strained at 300°K prior to tensile testing. The yield point observed under this latter condition is thought to be related to a mechanism suggested by Haasen and Kelly (38). Edwards, Phillips, and Liu (39) also observed similar yield point phenomena when they were trying to explain the yield point in steel. In studying the yield point in steel, they studied face-centered cubic metals and alloys and found that they could almost always develop a yield point by giving the specimens an appropriate thermomechanical treatment. Edwards, Phillips, and Liu observed that the alloys would develop yield points by subjecting them to quenching and aging treatments; but the pure specimens which had been simply quenched, or quenched and tempered, did not give any sign of yield point. In the specimens that were quenched, strained, and then tempered, however, quite distinct yield points were obtained. Haasen and Kelly (38) also investigated the yield point phenomena of aluminum and nickel, and observed that it would appear only after there had been previous plastic flow. They suggested that the effect is due to a rearrangement of dislocations during unloading which involves the pinning of dislocations. Stacking faults may be responsible for pinning the dislocations after they are formed by plastic flow. Gold has a low stacking fault energy which permits perfect dislocations to dissociate into partial dislocations. The width of the extended partials is controlled by the balance of their mutual repulsive force and the stacking fault energy. Thus, the greater the extension of the partials and the greater the number of extended dilocations, the more difficult it will be to move an unextended dislocation through a dislocation forest.

The recrystallization texture of the gold was determined after it had been heated to 1000°C and quenched to room temperature. The recrystallized texture was [100]. A study of the rotation of the fiber axis was made on a single wire that was aged for 800 hours at 100°C after various amounts of strain. The slip system found to be operating was (111) [110]. These results are presented in figure 29.

DISCUSSION

A. The Incubation Period and Temperature Recovery Ranges

The mechanisms of vacancy annihilation are related to the kinetics and the problems of nucleation. Whether or not stable clusters would form depends critically on the concentration of vacancies in excess of the equilibrium value. The equilibrium number of single vacancies in a gram-atom of metal is given by the expression

$$C = N \exp (-E_f / RT) \tag{5}$$

where E_f is the energy required to form a single vacancy, R is the universal gas constant, T is the absolute temperature, and N is Avagadro's number.

The kinetics of vacancy annihilation is complicated by the possibility of various vacancy associations with other imperfections (40). Vacancies can associate in pairs or in complexes containing i vacancies; they can become associated with edge dislocations, or with edge parts of complex dislocations. Vacancies can form atmospheres around dislocations at high temperatures, and they may also associate with substitutional atoms.

Formal thermodynamic theory of point defects allows one to calculate the equilibrium number of vacancy complexes. For example, the equilibrium number of divacancies is given by the equation

$$d = pc^2 \exp -(U/RT) \tag{6}$$

where p is a geometrical factor, c is the concentration of monovacancies, and U is the energy of association. Equation (6) can also be expressed in terms of the equilibrium number of single vacancies by the expression

$$d = pN^2 \exp -(2E_f - U)/RT \tag{7}$$

The problem of vacancy complex nucleation and the influence of the quenching rate, $-dT/dt$, on the number of complexes formed during the quenching period t_o will be considered. The theoretical quenching rate necessary to retain the equilibrium number of vacancies that exists at the temperature from which the specimen is quenched will be estimated. Several methods will be used to estimate the theoretical quenching rate.

It is necessary to show that the concentration change in the wire (cylinder of infinite length) is insignificant during the quenching period. In this case, we can consider the wire to be a cylinder of infinite length, and that diffusion occurs in the radial direction only. Darken (42) gives the following relationship

$$F = (\bar{c} - c_f)/(c_j - c_f) = 2.256 (Dt)^{1/2}/L \tag{8}$$

where $\bar{c}$ is the average concentration in the cylinder of radius L_o, whose initial uniform concentration had been c_j, while its final concentration is c_f. This latter expression is good for very short times. By assuming different values for t, values for L can be estimated. Values of L were computed using the coefficient of self-diffusion for gold at 1000°C. L values as a function of t_o are tabulated in table 3. The value for D can be determined from the relationship (43)

10

$$D = 1.26 \times 10^2 \exp \left(-51,000 / RT\right) \tag{9}$$

TABLE 3

AVERAGE DIFFUSION DISTANCE L OF VACANCIES
DURING THE QUENCHING PERIOD t_o

t_o (seconds)	L (Angstroms)
10^{-6}	24
10^{-4}	240
10^{-2}	2400
10^{-1}	7800

The values of L listed in table 3 represent an upper limit to the distance that a vacancy can diffuse during the quenching period, and these values indicate that the loss of vacancies due to radial diffusion to the surface of the specimen is negligible during the quenching period. Also of interest is the mean free path between vacancies whose concentration is 10^{-4} moles. The mean free path between collisions is approximately 1500 angstroms, if the equation applicable to gases can be used to estimate the distance in solids. A value can be estimated for the quenching period by comparing the mean free path between collisions to the results given in table 3. A value of order 10^{-4} seconds for t_o is required to retain the high temperature number of single vacancies at some lower temperature. Thus, the quenching rate necessary to have a t_o of order 10^{-4} would be of the order 10^{7}°C/sec.

In discussing the life time of a vacancy during the quenching period, it is useful to separate the effect of temperature by calculating the number of jumps n made by a vacancy during its life. The number of jumps n is given by the expression

$$n = AQ\mu t_o \exp \left(-E_m / RT\right) \tag{10}$$

where A is an entropy of activation and Q is the number of nearest neighbors. $\bar{n}$ is defined as the average number of jumps per second that a vacancy makes during the quenching period by the expression

$$\log \bar{n} = \log AQ\mu - E_m / 2R \left(T_q + T_o / T_q T_o\right) \tag{11}$$

or

$$\bar{n} = AQ\mu \exp \left[-E_m / 2R \left(T_q + T_o / T_q T_o\right)\right] \tag{12}$$

11

With T_q equal to 1273°K and T_o equal to 300°K, the value for $\bar{n}$ is equal approximately to 10^8 jumps per second. Table 4 gives some values for the number of jumps made by a vacancy during different quenching periods.

TABLE 4

NUMBER OF VACANCY JUMPS DURING A QUENCHING PERIOD

Quenching Rate	10^9°C/Sec	10^7°C/Sec	10^5°C/Sec	10^4°C/Sec
Time Constant, t_o	.000001	.0001	.01	.1
No. of Jumps, $\bar{n}t_o$	10^2	10^4	10^6	10^7

Table 4 shows that the average number of jumps made by a vacancy during the quenching period varies markedly with the quenching rate. It can be surmised that when a vacancy makes only 10^2 jumps during the quenching period, that it probably will not have disappeared at a sink, nor have diffused far enough to have made a collision with another vacancy. It is not likely that it would disappear at dislocations in gold, since the dislocations at high temperatures will be extended widely. Extended dislocations are poor sinks since they must be constricted before they can absorb vacancies. By making 10^4 jumps, the vacancies have probably formed a complex. Vacancy clustering is an inherent complication in quenching experiments due to the mutual encounter of the point defects during the quench. Substantial changes in the number of single vacancies can occur during the quench, if the association energy U is appreciable. If vacancies make 10^7 jumps during their life time as single vacancies, the number of single vacancies retained after the quench in excess of the equilibrium number at the lower temperature will be considerably reduced. Clustering will be very marked if the association energy U is greater than 0.2 ev. It has been suggested that the association energy for a pair of vacancies in gold is as much as 0.4 ev (45). The kinetics of the decay process is considerably complicated by the formation of the highly mobile divacancies and immobile stable clusters.

The occurrence of the three different temperature recovery ranges observed with the isochronal aging experiments is primarily due to the athermal clustering of vacancies. Athermal clustering of vacancies to form mobile complexes also accounts for Meshii and Kauffman (36) obtaining maximum saturated hardening of gold after aging for one hour at 100°C when the specimens had previously been quenched at 30,000°C per second. The gold specimens, quenched at a speed of 10^7°C/sec, had the highest temperature recovery range. This high temperature recovery range indicates that the species formed or retained due to the very short quenching period have the largest energy of migration. The defects which formed when the specimens were subjected to slower quenching speeds have lower energies of migration. Large numbers of divacancies could form during the longer time periods of the slow quenching speeds, and, since their energy of migration is about one-half the energy of migration of a single vacancy, cause the recovery range to be shifted to lower temperatures. The results of the isochronal aging experiments suggest that, with sufficiently rapid quenches, incubation periods can be expected to occur during isothermal aging experiments with those metals which can be quenched fast enough to retain large numbers of single vacancies.

One must be careful not to exceed the critical quenching speed, since plastic deformation may occur and many generate dislocation sinks for vacancies. Thermal stresses introduced into the wire by quenching can be computed by thermal-elastic theory. Formulae (56) for the radial and tangential stresses caused by a temperature gradient between the surface and the core of the wire are:

$$\sigma_r = \frac{E}{(1-\mu)} \left[-\frac{1}{r^2} \int_0^r \alpha \, T r \, dr + \frac{1}{b^2} \int_0^b \alpha \, T r \, dr \right] \tag{13}$$

$$\sigma_r = \frac{E}{(1-\mu)} \left[\frac{1}{r^2} \int_0^r \alpha \, T r \, dr + \frac{1}{b^2} \int_0^b \alpha \, T r \, dr - \alpha T \right] \tag{14}$$

where α is the thermal expansion coefficient, b is the radius of the wire, and T is the temperature distribution. E is the modulus of elasticity in the equations, and it is considered to be a constant. For accurate calculations of the thermal stresses, the temperature dependence of the elastic coefficients must be taken into consideration.

If the distribution of temperature over the radius of the wire is known, the integrals can be evaluated and σ_t and σ_r determined for each case. The maximum shear stress is given by

$$\tau_{max} = \frac{\sigma_\tau - \sigma_r}{2} \tag{15}$$

With a cosinusoidal temperature distribution

$$T = T_0 \cos \pi r / 2 b \tag{16}$$

where T_0 is the difference in temperature between the inside of the wire and the surface, we can express τ_{max} to be approximately

$$\tau_{max} = \frac{1}{5} \frac{E \alpha}{(1-\mu)} \frac{dT}{dt} \frac{b^2}{\delta} \tag{17}$$

where μ is Poisson's ratio, δ is the thermal diffusivity, and b is the radius of the wire. Table 6 presents some critical quenching speeds and critical radii of wires which were calculated using an expression similar to equation (17). Examination of the table shows that the radius of the specimen must not exceed the value of R in the table for a given quenching speed V_q, if no plastic deformation by thermal stresses is to occur. Some estimated values for thermal stresses in the gold wires are presented in table 5.

13

TABLE 5

THERMAL STRESSES IN 0.25 mm GOLD WIRE
AS A FUNCTION OF QUENCHING RATE

V (°C/sec)	τ_{max} (Kg/mm^2)
10^7	90
10^5	0.9
10^4	0.09

The thermal stresses in table 5 are only approximate, and they only represent an order of magnitude calculation. A similar calculation was made for platinum wires of 0.25 mm diameter; the calculated value for the maximum shear stress was approximately 0.6 Kg/mm^2. Neither gold nor platinum will exceed their yield strength when the quenching rate does not exceed 10^5°C/sec.

TABLE 6 (46)

CRITICAL QUENCHING SPEED AND CRITICAL RADIUS OF WIRES

Material	Heat Diff. (cm^2/sec)	Lin expansion coeff. α (°C)$^{-1}$ 10^5	V_{cr} at R=0.1mm (°C/sec)	V_{min} (°C/sec)	R_{cr} at $V_q=10^4$ °C/sec (mm)
Cu	1.00	1.8	1.7×10^4	$\approx 10^4$	0.13
Au	1.21	1.5	2.4×10^4	$\approx 10^4$	0.16
Ag	1.63	2.0	2.4×10^4	$\approx 10^4$	0.16
Al	0.92	2.8	1.0×10^4	$\approx 10^5$	0.10
Ni	0.14	1.6	0.8×10^4		0.09
Pt	0.23	1.0	2.1×10^4		0.15
Fe	0.10	1.5	0.6×10^4		0.08
Mo	0.52	0.5	1.95×10^4		0.31
W	0.62	0.5	1.1×10^4		0.33
Ge	0.28	0.7	12(R-1cm)	≈ 1	0.33
Si	0.42	0.3	42(R-1cm)	≈ 1	0.65

The value of V_q given in table 6 for gold is about one order of magnitude smaller than that actually required to observe an incubation period when the specimens are isothermally aged. There are other conditions in addition to the inherent physical constants which place a limit on the quenching speed. A limit is also placed on the quenching speed by the "Freeze-In Condition" of the metal. Some of the "Freeze-In" factors are sink density, defect diffusivity, and stacking fault energy.

It is reasonable to assume that vacancy clusters are formed by the mechanism whereby single vacancies are added one at a time to an embryo of size Z, and that the reaction is accompanied by a heat of reaction equal to the energy of association of the complex formed. Some typical reactions are represented by the following chemical type equations.

$$Z + q = B_{Z+1}$$

$$B_{Z+1} + q = B_{Z+2}$$

$$B_{Z+2} + q = B_{Z+3}$$
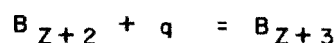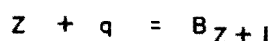
Each complex formed in the above manner will have an association energy which can be estimated by counting the number of V - V pairs in the cluster. The association energy U can be considered to be the sum of the V - V bond energies.

When the association energy is known for a particular complex, the equilibrium concentration as a function of temperature can be calculated using equations similar to (1), (2), and (3) of this section. Equilibrium concentrations of divacancies and trivacancies were calculated in this manner as a function of temperature, and they are presented in table 7.

TABLE 7

CONCENTRATION OF VACANCY COMPLEXES
AS A FUNCTION OF TEMPERATURE

Temp. ($^\circ$C)	100	300	500	700	900	1000
C_d (U)	$8.9\text{-}10^{-4}$	$3.5\text{-}10^{-5}$	$7.8\text{-}10^{-6}$	$3.2\text{-}10^{-6}$	$1.6\text{-}10^{-6}$	$1.3\text{-}10^{-6}$
$C_t(2U)$	$6.8\text{-}10^{-4}$	$1.2\text{-}10^{-6}$	$5.1\text{-}10^{-8}$	$8.3\text{-}10^{-9}$	$2.6\text{-}10^{-9}$	$1.5\text{-}10^{-9}$
$C_t(3U)$	10^{0}	$4.6\text{-}10^{-4}$	$4.6\text{-}10^{-6}$	$2.7\text{-}10^{-7}$	$4.6\text{-}10^{-8}$	$2.3\text{-}10^{-8}$

The concentration of vacancy complexes is a strong function of the excess number of single vacancies at any given reaction temperature. The values given in table 7 were determined by using the value for the concentration of monovacancies at 1000°C, since it was assumed that none would be lost during the quenching period.

A generalized equation for the concentration of vacancy complexes having i vacancies per complex is given by

$$C_x = P_j \, C_v^i \, \exp \, (mU/RT) \tag{18}$$

where P_j is a geometrical factor equal to the number of nearest neighbors divided by the number of vacancies in the complex i, and m is the number of V - V pairs. Different values for the association energy of vacancy pairs were tried, and it was observed that a value for U of slightly less than 0.3 ev would be a good estimate of the binding energy of divacancies in gold. The value of 0.4 ev reported by Meshii and Kauffman (45) appears to be slightly high. An association energy of 0.3 ev was used to calculate the concentrations presented in table 7. Although the calculated values of the various concentrations may be in error due to inaccurate values of E_f and U, they do illustrate that defect clusters are present in considerable numbers at intermediate and low temperatures which can nucleate when the quenching period is of appreciable duration.

The incubation periods observed for the isothermal aging curves of gold specimens quenched at a speed of 10^5°C/sec can be explained in terms of the percent of clustering achieved during the quenching period. Figures (23) and (24) show the incubation periods obtained for the aging experiments. The duration of the incubation periods was approximately one hour for an aging temperature of 200°C and about 16 hours for an aging temperature of 100°C. It should be further observed that the shape of the aging curves beyond the length of the incubation period is the same as that for platinum shown in figure 9, and the same as the aging curve determined for copper by Kimura et al (15). No incubation periods were observed for either copper or platinum specimens whose quenching rate was of the order 10^4°C/sec. The type of nucleation responsible for incubation periods can schematically be described by figures (30) and (31). Figure 30 is a generalized Time-Temperature-Nucleation plot combining both thermal and athermal nucleation characteristics. Figure 31 is a generalized Time-Temperature-Annihilation plot showing percent annihilated for a typical quenched and aged specimen. The T-T-N plot gives the number of nuclei present in the lattice as a function of time after instantaneous quenching to some temperature T from equilibrium at some fixed temperature near the melting point. The T-T-A plot gives the fraction of the vacancies annihilated as a function of time after an instantaneous quench to an arbitrary temperature T, from equilibrium at a fixed temperature near the melting point. The lines a, b, and c represent the time necessary to quench from the fixed temperature near the melting point to some arbitrary aging temperature T. The distance of the lines from the T-T-A curve is proportional to the incubation period encountered in an isothermal aging curve experiment.

The presence of an incubation period in the isothermal aging experiments and the different temperature recovery ranges observed during the isochronal aging experiments can be accounted for when the possibility of athermal nucleation is considered. The type of nucleation involved probably includes both thermal and athermal nucleation. A schematic picture of the combination nucleation mechanism is presented by means of a Time-Temperature-Nucleation plot, and the influence of the quenching rate on the degree of completion of the reaction is presented by a familiar Time-Temperature-Annihilation plot. The shape of the isothermal aging curve for gold and platinum beyond the incubation period will be discussed in the following section.

B. Mechanism of Quench Hardening in Platinum and Gold

The initial stage of the hardening mechanism was concerned primarily with the formation of vacancy complexes. This section is concerned with the product of the annihilation reaction and the mechanism by which the lattice is hardened.

It was observed that the maximum strength level after aging for the metals investigated was greater than the as-quenched strength by a factor of 2. Platinum showed evidence of overaging between 400° and 600°C. Gold did not show any sign of overaging at its maximum aging temperature of 200°C. Meshii and Kauffman (36) annealed out the quench hardening effects in gold in a temperature range close to 600°C.

Effective activation energies for the motion of point defects were calculated at different stress levels for platinum. When the yield strength reached a value of one half the maximum strength the activation energy was 0.69 ev, and the value at saturation strength was found to be 1.43 ev. Defects with different diffusivities are apparently involved in the diffusion process to form the defect structure which hardens the lattice. A spectrum of activation energies is involved. The effective activation energy increases as the aging progresses, Kappenal and Fine (23), and Wechsler and Kernohna (24) observed a similar behavior of the activation energies during investigations of quench aging in Cu-Al alloys. The defect which had the lowest activation energy and largest diffusivity annealed out first; thus, leaving the defect with the largest activation energy to anneal out last.

Several peaks were observed in the aging curves for platinum and gold at each temperature where the specimens were isothermally aged. The aging peaks were similar for both materials. The peaks can be seen in figures 8, 9, 23 and 24. The first aging peak for the platinum specimens was investigated by calculating effective activation energies at stress levels that were not too widely separated. The lowest stress levels correspond to very short aging times. After a short aging time, the activation energy was calculated to be 1.28 ev, which is about the activation energy expected for the migration of divacancies. An activation energy for a longer time was calculated to be 1.33 ev; this value corresponds to the activation energy for the migration of single vacancies. The spectrum of activation energies obtainable explains why the decay kinetics are very complex.

The type of defect structure formed as a product of the annihilation process is fundamentally controlled or explained by one characteristic property of the metal--its stacking fault energy. The latter statement is true when the concentration of vacancies is relatively high. When vacancies combine to form clusters that eventually become immobile, the cluster condenses out on the {111} planes. The {111} family of planes has the closest packing of all the crystal planes and possesses more sites for the nucleation of clusters. The stacking fault energy determines whether the planes will collapse.

The possibility that the vacancies frozen into the lattice on quenching from high temperatures coalesce to form plate-shaped regions on the closest-packed planes has been discussed by several authors. Kimura et al., (15) (21) pointed out that the coalescense of vacancies on the {111} planes depended on quenching the specimen from a temperature very near the melting point. The excess vacancies which are in the forms of divacancies and trivacancies act as nuclei for the formation of clusters which grow, collapse on {111} planes, and finally give rise to dislocation rings. The dislocation ring surrounds an area of stacking fault. The defect is described as Frank Partial dislocation or a sessile dislocation having a Burgers vector $b = a/3$ [111]. Such a defect is not free to move in its

slip plane which provides a means for the pinning of dislocations. The sessile dislocation may provide a pinning mechanism for screw dislocations (21), and may possibly explain the rise to the second peak of the annealing curves.

The minimum which occurs between the two aging peaks may be related to the excess concentration of vacancies in the lattice. In general, there exists some mutual interaction between dislocations and vacancies. At thermal equilibrium, atoms join and leave jogs with equal frequency. However, when there is an excess number of vacancies in the lattice, the rate of arrival of vacancies at the jogs increases and the extra plane of atoms shrink. This is dislocation climb for which the excess vacancies in the lattice are a driving force. The critical stress for rapid climb is decreased because the energy of vacancy formation does not have to be supplied by an applied stress. Climb increases the macroscopic strain of a crystal when a tensile stress is applied, that is, it encourages it to elongate. When the average elongation of the platinum specimens was observed to increase, the yield strength correspondingly dropped giving the minimum in the yield strength versus aging time plot.

The gradual rise in the yield strength-aging time plot after the second aging peak for platinum and gold can qualitatively be explained by considering the mechanism by which adjoining close-packed planes collapse after the condensation of vacancies has occurred on these planes. Two different kinds of dislocations can be distinguished. If a displacement vector joins two identical atom positions in the structure, it is possible to fill in or take away atoms so as to recreate perfect crystals everywhere except near the dislocation line. If the displacement vector does not join identical atom positions, then a surface fault will remain. The dislocation line which forms the boundary of the faulted area is called an imperfect dislocation.

Read (15) pointed out that the {111} planes can collapse in two ways: (1) two adjoining planes can come together without offset and produce a one-layer fault surrounded by a negative Frank Partial (sessile) dislocation, and (2) atomic planes could come together with an offset with a relative displacement of $a/2[011]$. This is accomplished geometrically by removing a B plane of face-centered cubic stacking and shifting all the planes above it so that a configuration $C \rightarrow B \rightarrow A \rightarrow C \rightarrow A$ is achieved. This displacement eliminates any fault, and the missing plane is surrounded by a closed loop of dislocation. Kuhlmann-Wilsdorf (35) also discussed the collapse of the {111} planes to form a disc of faulted material surrounded by a sessile dislocation with a Burgers vector of $a/3<111>$. This loop can neither glide nor act as a dislocation source since the vector lies outside the plane of the loop. Kuhlmann-Wilsdorf pointed out that such an arrangement is unstable with metals having a large stacking fault energy. Energy-wise it may be more favorable to nucleate a shockley partial, which lies in the same octahedral plane, on the faulted area and combine it with the loop dislocation according to the reaction

$$a/3 \left[111 \right] + a/6 \left[\bar{2}11 \right] = a/2 \left[011 \right]$$

This dislocation was called an "R-dislocation" by Kuhlmann-Wilsdorf.

The stability condition for a circular "R-dislocation" of radius ρ can be estimated by using the equation derived by Kröner (48) for the energy of a dislocation ring with and without a stacking fault. The energy of a dislocation ring with a stacking fault is

$$E_1 = 2/3 \frac{1}{(1-\mu)} + Gb^2 \rho \left[\ln \left(\frac{\rho}{\rho_0} \right) - 1 \right] - \pi \rho^2 \gamma \tag{19}$$

The energy of the "R-dislocation" is

$$E_2 = 2/3 \frac{1}{(1-\mu)} + 1/3 \frac{(2-\mu)}{2(1-\mu)} Gb^2 \rho \left[\ln \left(\frac{\rho}{\rho_0} \right) - 1 \right] \tag{20}$$

The criterion for the "R-dislocation" to be more stable than the defect structure with the fault is

$$E_1 \geq E_2 \tag{21}$$

The "R-dislocation" will be stable when

$$\gamma \geq \frac{Gb^2}{3\pi} (0.595) \frac{1}{\rho} \left[\ln \left(\frac{\rho}{\rho_0} \right) - 1 \right] \tag{22}$$

An estimate of the ring radius ρ belonging to an "R-dislocation" can be made when values of γ, G, b, ρ, and μ are known. Some values of ρ were calculated for face-centered cubic metals having different stacking fault energies. The values are presented in table 8.

TABLE 8

ESTIMATED VALUES OF ρ FOR SOME
FACE-CENTERED CUBIC METALS AT 300°K

Metal	Au	Ag	Pt	Cu	Ni	Al
G x 10″	2.5	2.6	5.0	4.2	8.3	2.7
b x 10^{-8}cm	2.88	2.88	2.78	2.56	2.49	2.86
ρ_0 x 10^{-8}cm	2.34	2.38	2.26	2.08	2.08	2.32
γ ergs/cm^2	17	31	35	58	74	78
ρ x 10^{-8}cm	1200	600	1075	375	617	180

The stacking fault energies were estimated from values derived as a function of temperature by Gegel and Speiser (37). Values of γ as a function of temperature are presented in figure 32.

The results presented in table 8; indicate that the radius for gold is so large that an "R-dislocation" could not occur spontaneously. The values for copper and aluminum are

in contrast to gold. The result for nickel is quite different from what is expected when the stacking fault energies are compared. The nickel ring size indicates that it should behave similarly to silver. Markovsky and Cherney (47) investigated structural changes in nickel during cold welding and found that the plastic deformation which takes place leads to the formation of nickel with a hexagonal lattice. This observation indicates that the large value calculated for the faulted area, which has a hexagonal structure, may not be unreasonable. Wyckoff (49) reports that two close-packed modifications exist for nickel, and that the hexagonal structure is thermodynamically more stable at room temperature. The energy associated with the two close-packed modifications is nearly the same, and there is little tendency to change from one to the other. The modification in nickel behaves like the metal cobalt. The F.C.C. structure of nickel will transform to the H.C.P. structure within several days at 170°C.

Platinum occupies a position between silver and gold since its stable ring size is intermediate to these metals. The difference in stacking fault energies does not entirely explain its behavior in recovery, since the stacking fault energy for platinum is not too different from that for silver. In quenched silver, both stacking faults and dislocation rings without stacking faults have been observed. However, the defect structure for platinum has not been studied. Silcox and Hirsch (50) observed a high density of loops in irradiated copper; it thus appears that silver is the border line case where one observes both dislocation loops with stacking faults and dislocation loops without stacking faults.

The resoftening process has been investigated for some of these materials. Meshii and Kauffman (36) observed that the yield strength in gold anneals out rapidly in a temperature range around 600°C, and that the activation energy was too high for self-diffusion to be the controlling process. Kino (51) observed softening in quench-hardened aluminum between 100° and 200°C, and Silcox (52) also observed dislocation loops in aluminum annealing out in this temperature range. Kimura, Maddin, and D. Kuhlman-Wilsdorf(15) (21) observed softening in copper around 100°C, and Silcox and Hirsch (50) observed the disappearance of loops in irradiated copper in the temperature range where recovery occurred. The quench-hardened platinum specimens were observed to anneal out between 400° and 600°C in this work. The recovery observed in the quench hardened materials is accompanied by an activation energy.

An activation energy of 1.43 ev was determined for the recovery process in platinum. The value of the activation energy will be determined by the specific hardening mechanism. From the results of the experiments, the hardening mechanism for platinum can only be speculated. By assuming that the stacking fault energy will be the factor in determining the hardening and recovery mechanism, a reasonable hardening mechanism can be proposed. Platinum occupies a position between silver and gold. Only dislocation rings having stacking faults and stacking fault tetrahedras have been observed in gold. In the case of silver, both dislocation rings and dislocation rings with stacking faults have been observed. The primary hardening mechanism in platinum appears to be the formation of sessile dislocations on the octahedral planes. Hardening will be a result of the interaction of the glide dislocations with the sessile dislocations to form jogs. Recovery begins to occur in the temperature range between 400° to 600°C. The recovery mechanism will involve the rearrangement of dislocations and wiping out the stacking fault area. The activation energy of the mechanism is less than the activation energy for self-diffusion. A first approximation to the estimation of the activation energy would be to consider the energy necessary to constrict screw and edge dislocations. The constriction of an extended dislocation would eliminate the faulted area. Thus, a first order approximation of the activation energy would be

$$\Delta H = E_s + E_e \tag{23}$$

The constriction energies, E_s for the dissociated screw dislocation and E_e for the dissociated edge dislocation, are not readily available for all F.C.C. metals. These constriction energies are a function of the stacking fault energies of the metals. Seeger (48) reported some values for Al, Cu, Ni, and Au which were calculated using some revised values of the stacking fault energies for the various metals. The values for E_s and E_e are probably too high, since the stacking fault energies for these metals at 300°K are approximately 50% less than the values which were used in the calculations. However, if the ratio of E_e/E_s is determined for each of the metals, one observes that an average value of this ratio is 3.15 to 1.

The stacking fault energies for the various metals is proportional to 1/x, the reciprocal of the equilibrium distance between extended partial dislocations. The latter relationship is readily observed from the expression for the equilibrium spacing of partials.

$$F_s + F_e + F_f = 0 \tag{24}$$

Where F_s is the energy of a screw component, F_e is the energy of an edge component, and F_f is the energy of a stacking fault equal to $-\gamma$.

$$F_s = G (b \sin 30)^2 / 2 \pi x \tag{25}$$

$$F_e = G (b' \cos 30)^2 / 2 \pi (1-u) x \tag{26}$$

$$x \approx F(b^2) / 9\gamma \approx Ga^2 / 54 \gamma \tag{27}$$

The activation energy should also be proportional to the width of the extended dislocations. An empirical relationship can be written to express these relationships. The expression is

$$K' \Delta H \gamma = a \; constant \tag{28}$$

where k' is the conversion factor for electron volts to ergs. Assuming that the activation energy for copper is best known, the constant in Equation (28) can be evaluated. Some estimated values for E_s, E_e, and ΔH are made and compared to some experimental values.

TABLE 9

SOME ESTIMATED AND MEASURED RECOVERY ACTIVATION
ENERGIES FOR VARIOUS F.C.C. METALS

Metal	Au	Pt	Cu	Ag	Ni	Al
E_s (est.) (ev)	0.60	0.35	0.17	0.32	0.15	0.13
E_e (est.) (ev)	1.85	0.55	0.55	1.02	0.48	0.39
ΔH (est.) (ev)	2.45	1.26	0.72	1.34	0.57	0.54
ΔH (meas.) (ev)	4.7	1.43	0.72	>1	0.63	0.52
References	36	53,31	15,21	6	10	8

Taranto and Brotzen (53) found evidence in support of the platinum model for lattice hardening. Using an X-Ray diffraction technique to determine stacking fault probabilities after various annealing treatments, they determined the activation energy for the disappearance of stacking faults in cold-worked platinum. Their analysis yielded an activation energy of 1.25 ± 0.34 ev. This recovery activation energy is much less than the activation energy for self-diffusion, which is 2.68 ev. If the recovery mechanism was due to the annihilation of dislocation jogs, the activation energy would be of the order for self-diffusion. Broad reflection lines became sharper early in the recovery process in their diffraction patterns before the stage during which the stacking faults completely disappeared. This condition lends support to the belief that a considerable rearrangement of dislocations takes place in the early stages of recovery.

The measured value for the activation energy for recovery in gold consists of the sum of the energy terms for the constriction of edge and screw dislocations plus the activation energy of self-diffusion. The activation energy for self-diffusion in gold is 2.2 ev. The sum of the energy terms for constriction in gold was estimated to be 2.45 ev. Thus, the sum of these terms is

$$\Delta H_{Au} = \Delta H_{sd} + E_s + E_e \qquad (29)$$

and the sum of these terms is 4.65 ev. The model for recovery in gold must be the elimination of extended sessile dislocations and the subsequent evaporation of vacancies from the stacking fault.

For the other metals considered in table 8 it appears that dislocation loops are the primary cause of lattice hardening. Smallman (55) points out that electron transmission studies indicate that helices appear to nucleate first and that the loops follow by a breakdown of the helices. The loops, if really nucleated from the helices, would consist of components of both screw and edge dislocations. In view of the activation energies measured for the recovery process, it can be concluded that the activation energy for recovery for Al, Ni, Cu, and Pt is the sum of the energy terms for dislocation constriction.

Examination of the slip lines for gold and platinum showed them to be long, sharp, and straight with cross-slip in evidence. The Laue patterns taken after fracture showed very little, if any, asterism. The quench-hardened specimens showed a very low rate of work

hardening. These facts indicate that the deformation process was nonturbulent in nature. In the case of gold, the slip system found to be operating was ($\bar{1}$11) [110]. An equivalent system for platinum was probably operating. The rotation of the fiber axis was followed in one of the gold specimens that had been fully hardened. The stereographic triangle is presented in figure 29. Frank partials and loops on a slip plane will act as a barrier to the generation of dislocations. The generation of dislocations by a source on the slip plane is hindered by the Frank partials and dislocation loops, since they limit the distance that the dislocations can move. The result is a pile-up of dislocations against the barrier. A back stress builds up and cancels some of the stress acting on the dislocation generator. Barriers on the primary slip system produce latent hardening on the secondary slip system (26). The amount of work hardening in a metal is dependent on the amount of intersection of the dislocations from the primary slip system with those on the secondary slip system. The back stress on the primary slip system probably has a component which raises the critical resolved shear stress on the secondary slip system. The proportional limit was measured for the gold specimens isothermally aged at 100°C. The change of the proportional limit with aging time is presented in figure 25. It was observed that the proportional limit was a minimum in the region of the curve where the relative maxima and minima occurred, and it was also observed to increase to a maximum value in the region where the specimens became fully hardened. This evidence lends support to the belief that the critical resolved shear stress on the secondary slip system has increased.

A feature of interest in the stress-strain curves for gold was the appearance of serrations in the curve after the specimens had been held for several minutes at the aging temperature, and occasionally one would find a yield point after several hours of aging. Prestraining the fully aged specimens prior to tensile testing also developed a yield point. A. T. Thomas made similar observations on Al-3%Cu alloys which were air cooled. He did not observe any serrations in the stress-strain curves for the specimens which had been water quenched in the as-quenched condition. There was a delay of 3% strain in these specimens before the serrations would begin to appear. In the case of gold, rapid quenching caused an incubation period to occur in the aging curve which was attributed to the prevention of clustering during the quenching period. Slowly quenched specimens did not exhibit an incubation period. Since the as-quenched specimens must be thermally treated or plastically strained before the serrations appear in the stress-strain curves, it seems reasonable to believe that the dislocations are pinned by vacancy clusters rather than by single vacancies. Similar to strain aging experiments, a certain amount of time will be necessary for the pinning species to diffuse to the dislocations. A divacancy complex has a larger diffusivity value than a monovacancy, and it could diffuse much faster to the dislocation line. From a geometrical point of view, the monovacancies would not cause the lattice to be strained very much and its interaction energy would not be sufficient to pin the dislocation. In the case of a substitutional alloy, the solute atom will not necessarily pin a dislocation. Excess vacancies can promote short-range ordering in substitutional alloys which is effective in dislocation blocking or locking.

CONCLUSIONS

Some major conclusions to be drawn from the results of this program are:

(1) Nucleation of vacancy complexes occurs during the quenching period when the average quenching speed is less than some critical value for the particular metal.

(2) The order of the decay kinetics is related to the type of vacancy complex reacting with single vacancies.

(3) Very few vacancies are lost to dislocations in F.C.C. metals which have low stacking fault energies, since the energy of constriction must first be overcome.

(4) The activation energy for recovery of quench-hardened F.C.C. metals, whose stacking fault energies are equal to or greater than that for platinum, is equal approximately to the sum of the constriction energies for screw and edge dislocations.

(5) The activation energy for recovery consists of the activation energy for self-diffusion plus the sum of the dislocation constriction energies for those metals whose attacking fault energies are less than that for platinum.

(6) In platinum, quench-hardening appears to be due to the formation of dislocation passage and cause dislocation pile-ups. The back stress from a pile-up probably increases the critical resolved shear stress on the secondary slip systems.

(7) In gold, quench-hardening is probably caused by the interaction of dislocations with stacking fault tetrahedra. Again, latent hardening on the secondary slip systems is probably due to back stresses of dislocation pile-ups.

(8) Dislocation clusters can interact with dislocations during plastic deformation to cause yield points or serrated stress-strain curves.

SUGGESTIONS FOR ADDITIONAL WORK

The implications of some of the results from this program have raised many questions. It is clear that work must be done to clarify the nature of the imperfections which are responsible for the change in the yield strength of the metals studied after various aging treatments. Electron transmission studies should be made after various times to follow the progress in the structural change. Thin films should be strained while in the electron microscope to determine the cause of latent hardening of the secondary slip systems.

Theoretical calculations should be made to improve upon the values for the energies of constriction for screw and edge dislocations. Since these energies are closely related to the stacking fault energy of the metal involved, theoretical and experimental work

must be done to obtain more reliable values and to prove that the stacking fault energy is a function of temperature for both metals and alloys.

Nickel should be investigated more thoroughly to determine if an allotropic transformation really does exist near room temperature. If one does exist, an explanation may be provided to clarify why, under certain conditions, it has a high value for its stacking fault energy; and why, under other conditions, it appears to have a low value.

REFERENCES

1. J. W. Kauffman and J. S. Koehler, Phys. Rev., 88. (1952), 149.

2. B. G. Lazarev and O. N. Ovcharenko, Dolk-Akad Nauk SSSR, 100, (1955), 875.

3. F. J. Bradshaw and S. Pearson, Phil. Mag., 1, (1956), 812.

4. G. L. Bacchella, E. Germegnoli and S. Granata, Jnl. Appl. Phys., 30, (1959), 748.

5. F. J. Bradshaw and S. Pearson, Phil. Mag., 2, (1957), 379.

6. J. A. Manintveld, Nature, 169, (1952), 623.

7. F. J. Bradshaw and S. Pearson, Phil. Mag., 2, (1957), 570.

8. W. DeSorbo and D. Turnbull, Acta Met., 7, (1959), 83.

9. C. Panseri, F. Gatto, and T. Federighi, Acta Met., 5, (1957), 50.

10. T. Broom, Advances in Physics, 3, (1954), 26.

11. R. O. Simmons and R. W. Balluffi, Phys. Rev., 119, (1960), 600.

12. R. O. Simmons and R. W. Balluffi, Phys. Rev., 117, (1960), 52.

13. R. O. Simmons and R. W. Balluffi, Phys. Rev., 117, (1960), 62.

14. J. J. Jackson, Ph. D. Thesis, University of Illinois, (1960).

15. H. Kimura, R. Maddin, and D. Kuhlmann-Wilsdorf, Acta Met., 7, (1959), 145.

16. C. Hsien Li, J. Washburn, and E. R. Parker, Jnl. Metals, 5, (1953), 1223.

17. R. Maddin and A. H. Cottrell, Phil. Mag., 46, (1955), 735.

18. J. Takamura and S. Miura, Bulletin, Spring Meeting, Japan Inst. of Metals, 38, (1956), 20.

19. M. Meshii and J. W. Kauffman, Acta Met., 7, (1959), 180.

20. T. Mori, M. Meshii, and J. W. Kauffman, Acta Met., 9, (1961), 71.

21. H. Kimura, R. Maddin, and D. Kuhlmann-Wilsdorf, Acta Met., 7, (1959), 154.

22. R. Maddin, A. H. Cottrell, Phil. Mag., 46, (1955), 1021.

23. T. J. Kappenaal, M. E. Fine, "Quench-Aging in Alpha Cu-Al Alloys," Report, Dept. of Materials Science, The Technological Institute, Northwestern University, Evanston, Illinois.

24. M. S. Wechsler, R. H. Kernohna, Acta Met., 1, (1959), 599.

REFERENCES (Continued)

25. W. T. Read, Jr., "Dislocations in Crystals," McGraw-Hill Book Co., Inc., (1953).

26. R. D. Heidenreich and W. Shockley, "Report of a Conference on Strength of Solids," Phys. Society, (1948), 57.

27. G. R. Piercy, R. W. Cahn, and A. H. Cottrell, Acta Met., 3, (1955), 331.

28. L. E. Tanner and R. Maddin, Acta Met., 2, (1959), 69.

29. R. A. Dugdale, Phil. Mag., 5, (1950), 201.

30. A. Ascoli, M. Asdente, E. Germagnoli, A. Manara, Jnl. Phys. and Chem. of Solids, 6, (1958), 59.

31. G. R. Piercy, Phil. Mag., 5, (1950) 201 .

32. American Inst. of Physics, "Temperature, Its Measurement and Control in Science and Industry, New York," Reinhold, (1941).

33. J. C. Fisher, J. H. Hollomon, and D. Turnbull, Jnl. Appl. Phys., 19, (1948), 275.

34. R. Maddin, C. H. Mathewson, and W. R. Hibbard, Jr., Trans. A.I.M.E., 185, (1949), 572.

35. D. Kuhlmann-Wilsdorf, Phil. Mag., 3, (1958), 125.

36. M. Meshii and J. W. Kauffman, Phil. Mag., 5, (1960), 939.

37. H. Gegel and R. Speiser, Unpublished Work.

38. P. Haasen and A. Kelly, Acta Met., 5, (1957), 192.

39. C. A. Edwards, D. L. Phillips, and Y. H. Liu, Jnl. Iron and Steel Inst., 147, (1943), 145.

40. H. Brooks, "Lattice Vacancies and Interstitials in Metals," Impurities and Imperfections, American Society for Metals, Cleveland, (1955), 1.

41. W. Jost, "Diffusion in Solids, Liquids, Gases," 3rd Ed., Academic Press Inc., (1960).

42. L. S. Darken and R. W. Gurry, "Physical Chemistry of Metals," McGraw-Hill Book Co., Inc., (1953), 447.

43. R. M. Barrer, "Diffusion in and Through Solids," Cambridge Univ. Press, Cambridge, (1951).

44. W. Bauerle, A. Klabunde, and J. S. Koehler, Phys. Rev., 102, (1956).

REFERENCES (Continued)

45. M. Meshii and J. W. Kauffman, Tech. Report No. 4, Contract NONR 1228(12), Project No. 031-613, Northwestern University, Evanston, Illinois.

46. H. G. van Bueren, "Imperfections in Crystals," 2nd Ed., North-Holland Publishing Co., (1961).

47. E. A. Markovsky and V. G. Cherny, Ukrain. Fiz. Zhur., (5), 5, (1960), 687.

48. A. Seeger, R. Berner, and H. Wolf, Zeitschrift für Physik, 155, (1959), 247.

49. R. W. G. Wyckoff, "Crystal Structure," Sec. I, (1948), 4.

50. J. Silcox and P. B. Hirsch, Phil. Mag., 4, (1959), 72.

51. T. Kino, Jnl. Sci. Hiroshima Univ., (A), 22, (1958), 259. Referenced in Jnl. Inst. Metals, 81, (1961), 303.

52. J. Silcox and M. J. Wheland, Phil. Mag., 5, (1960), 1.

53. J. Taranto and F. R. Brotzen, Trans. A.I.M.E., 221, (3), (1961), 645.

54. A. T. Thomas, Jnl. Inst. Metals, 81, (1961), 305.

55. R. E. Smallman, Jnl. Inst. Metals, 81, (1961), 306.

56. S. Timoshenko, "Strength of Materials," Part II, D. Van Nostrand Co., Inc., 3rd Ed., (1956), 228.
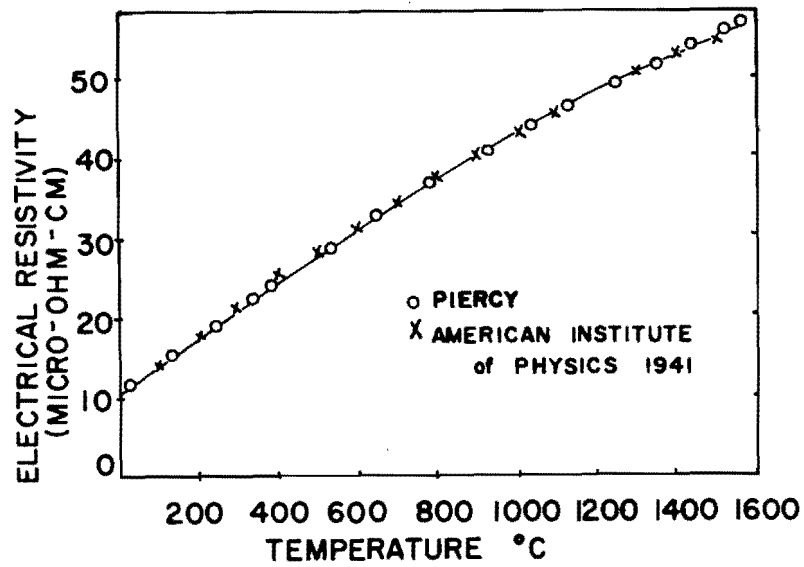
Figure 1. Resistivity of Platinum as a Function of Temperature
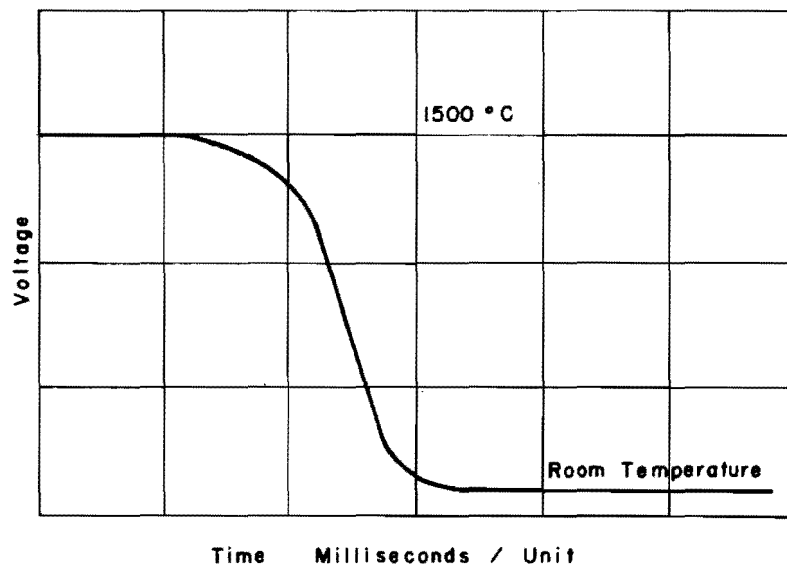
Figure 2. Typical Quench Curve for Platinum
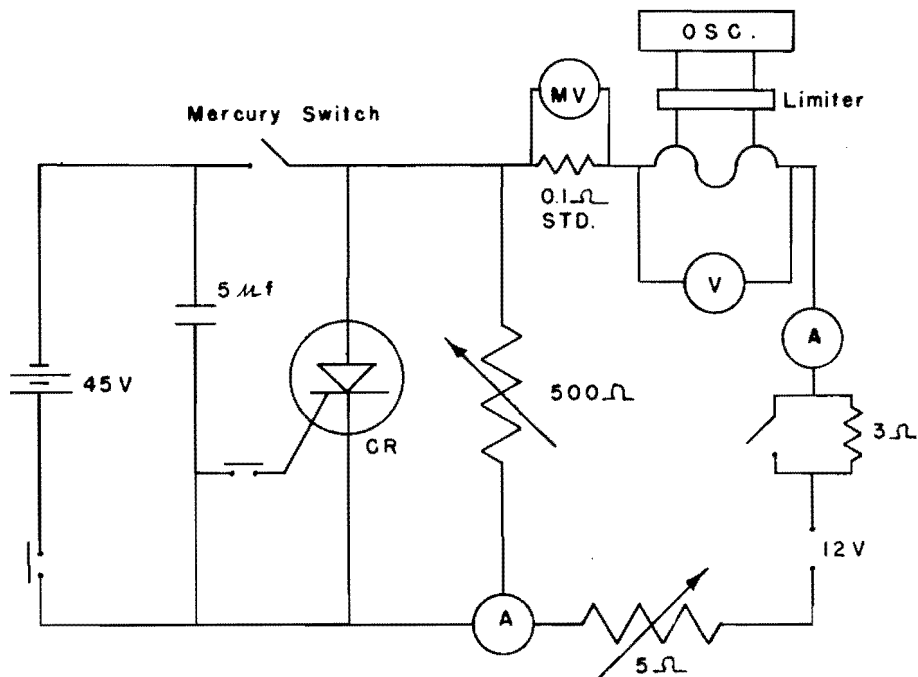
Figure 3. Schematic Drawing of the Heating and Quenching Circuit
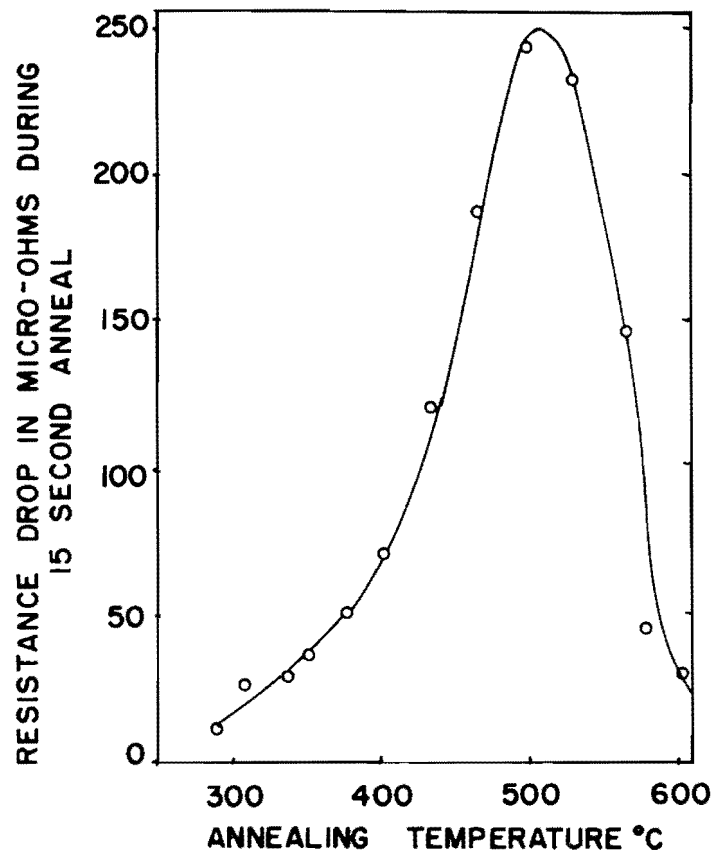
Figure 4. Piercy's Isochronal Resistivity Curve for Platinum
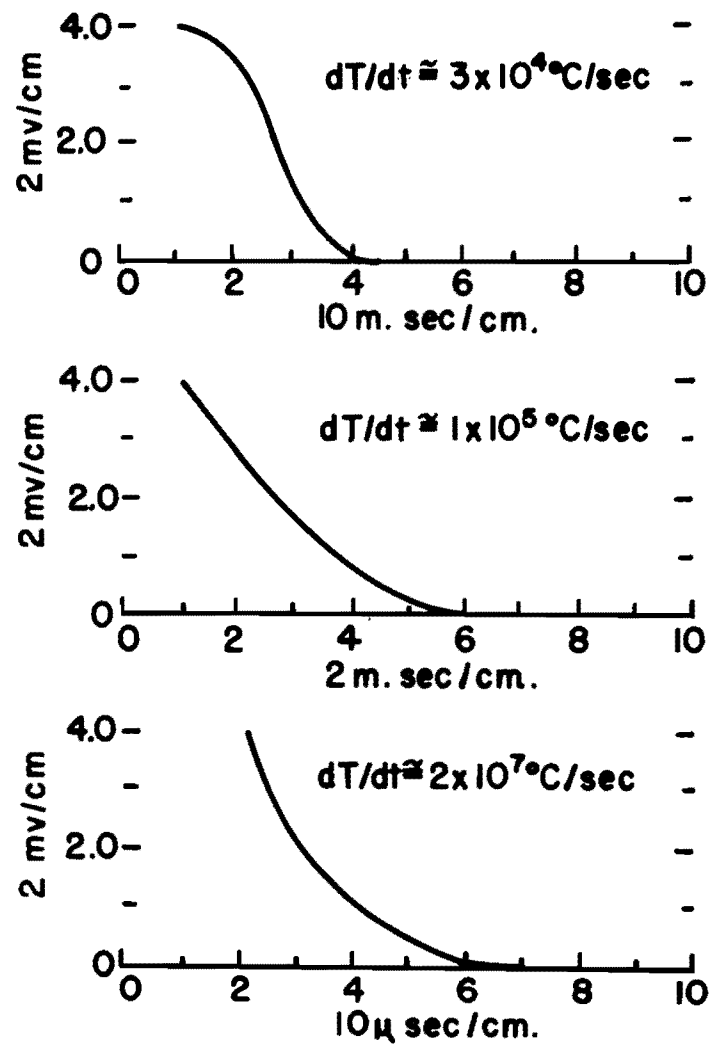
Figure 5. Quenching Rate Curve for Gold Wires Quenched into Different Medias
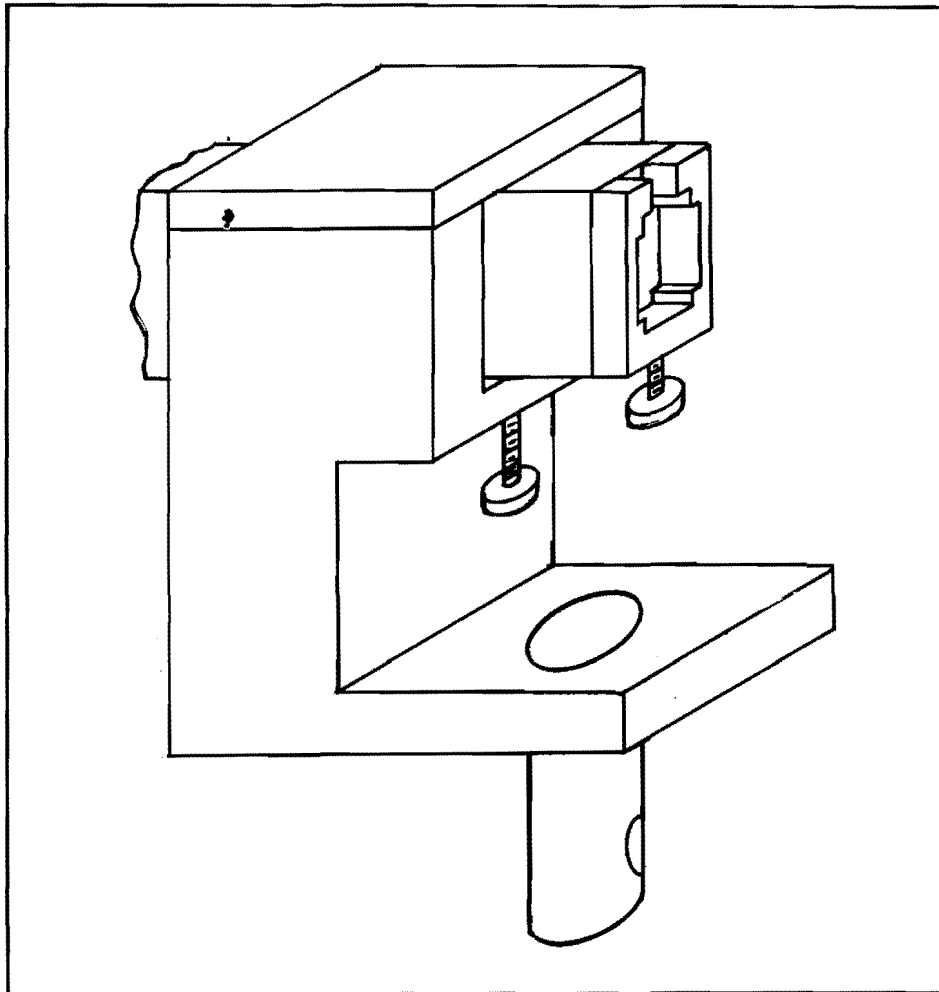
Figure 6. Specimen Grip Holder
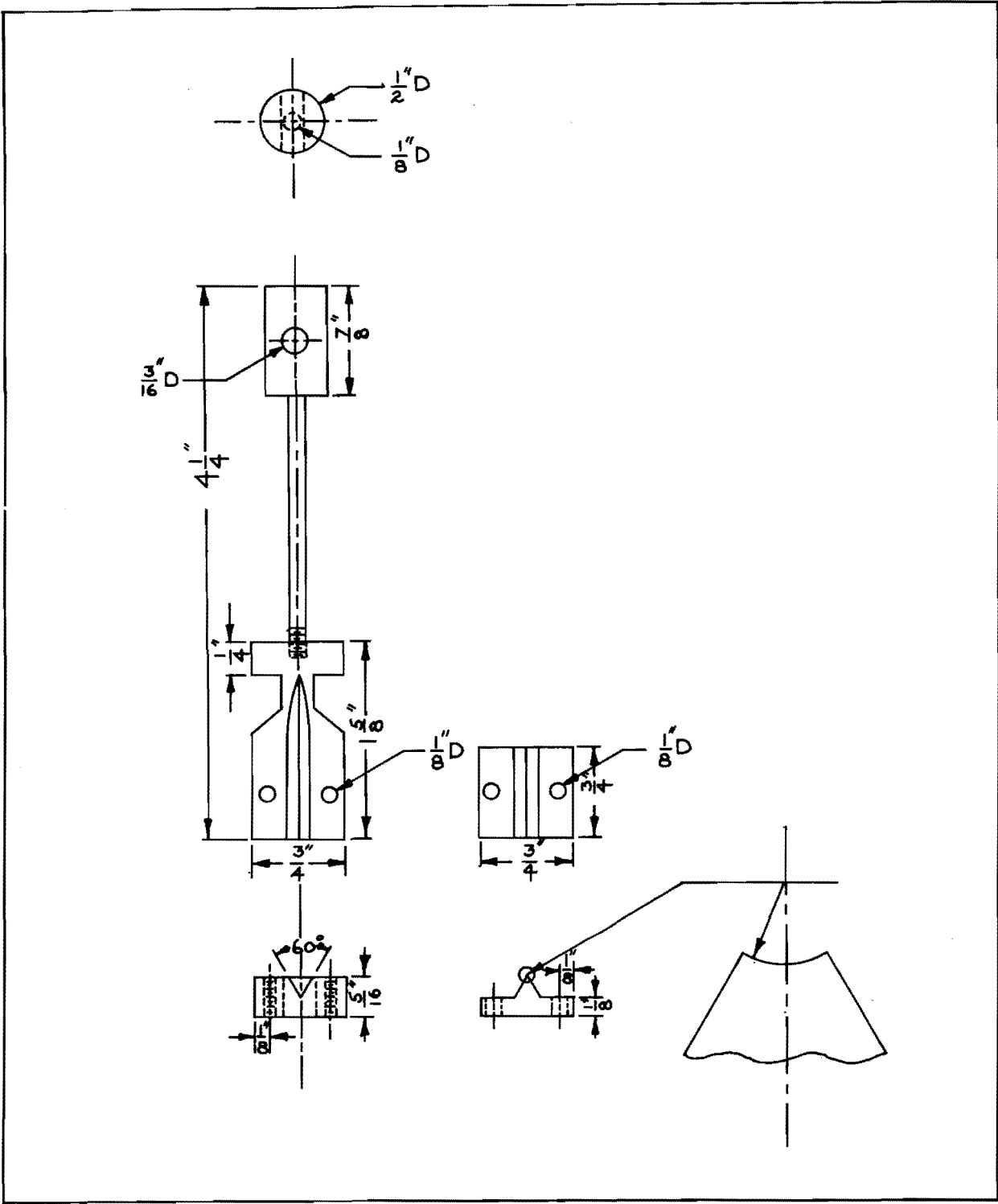
Figure 7. Wire Tensile Grips
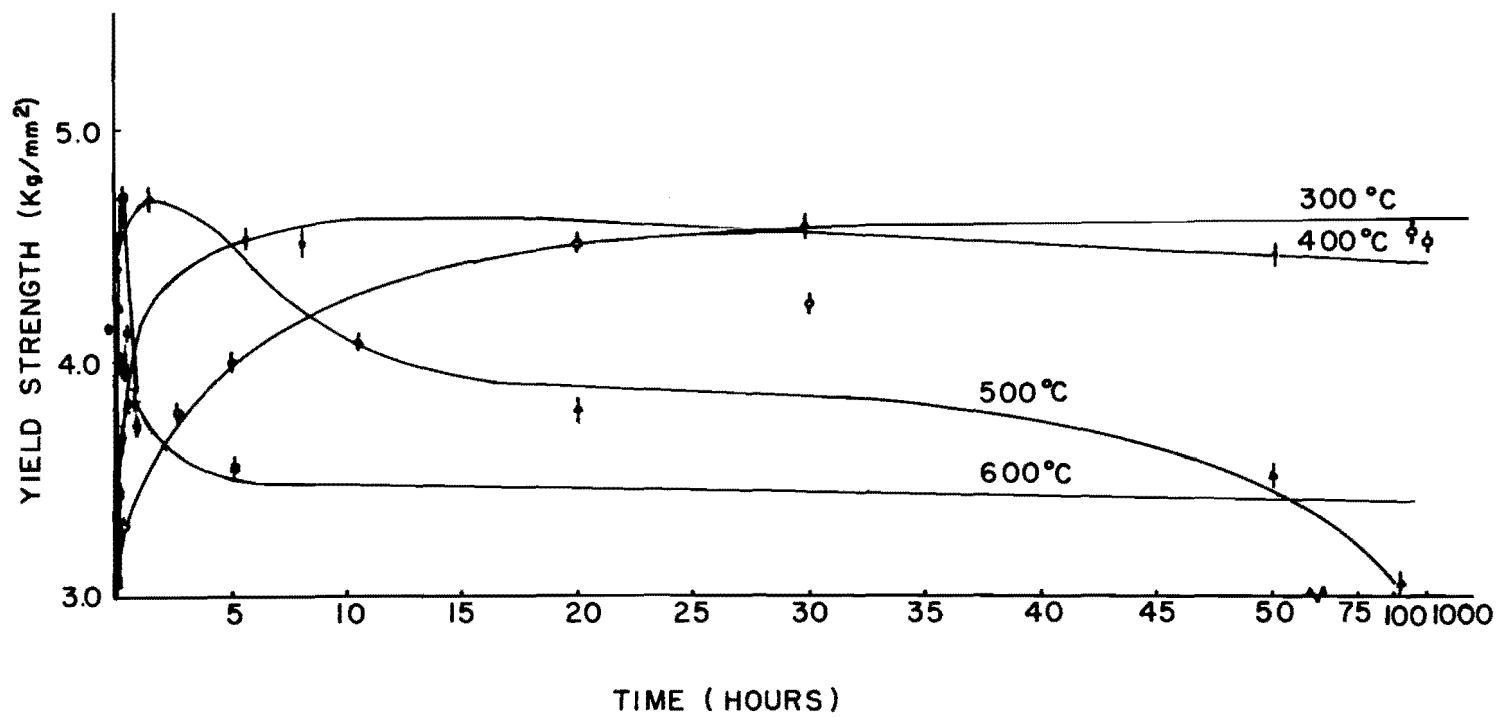
Figure 8. Long Time Isothermal Aging Curve for Platinum
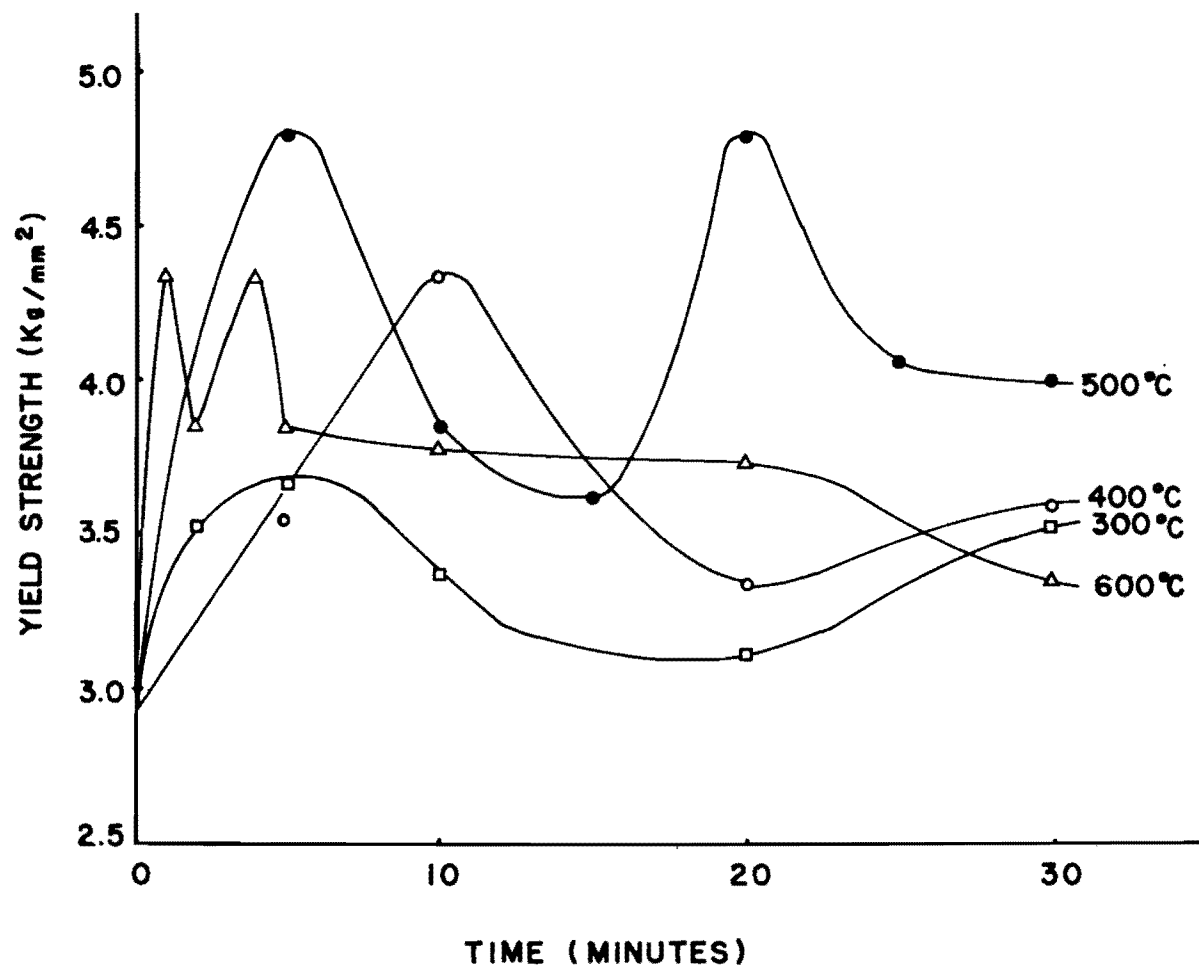
Figure 9. Short Time Isothermal Aging Curve for Platinum

—
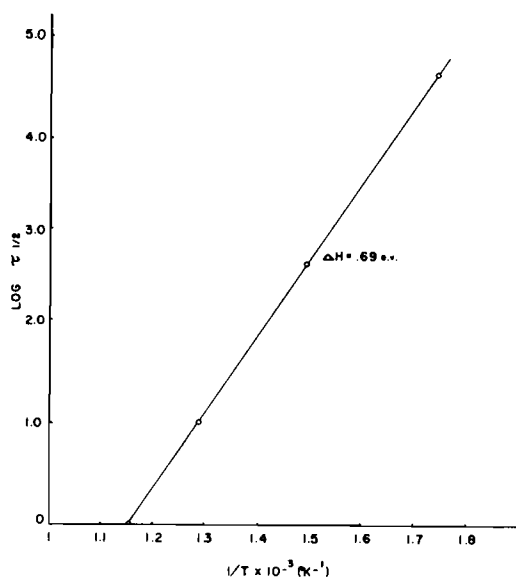
Figure 10. Plot of Log $\tau_{1/2}$ Versus $1/T_a$ for the Recovery Process in Platinum
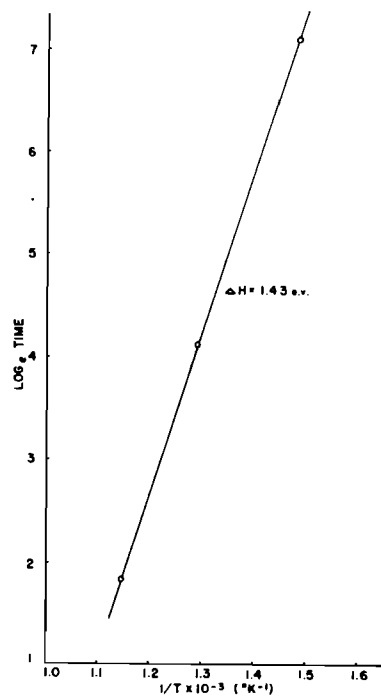
Figure 11. Plot of Log Time Versus $1/T_a$ for the Recovery Process in Platinum
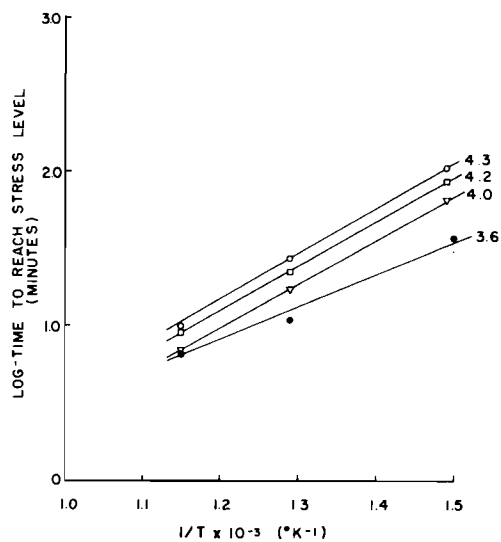
Figure 12. Plot of Log Time Versus $1/T_a$ for Four Different Stress Levels for Platinum
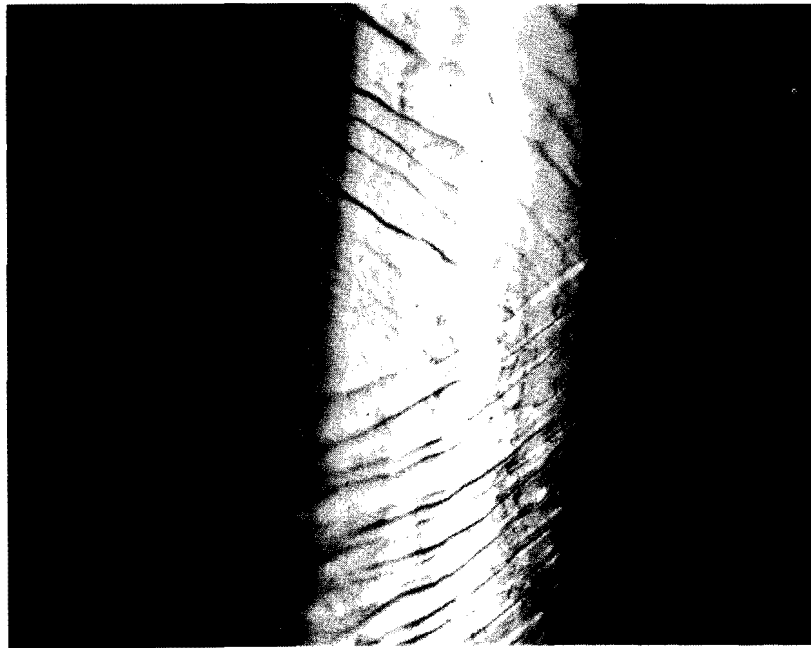
Figure 13. Cross-Slip in Platinum Wire 450X

Figure 14. Slip Lines in Platinum Wire in a Necked Down Region 720X
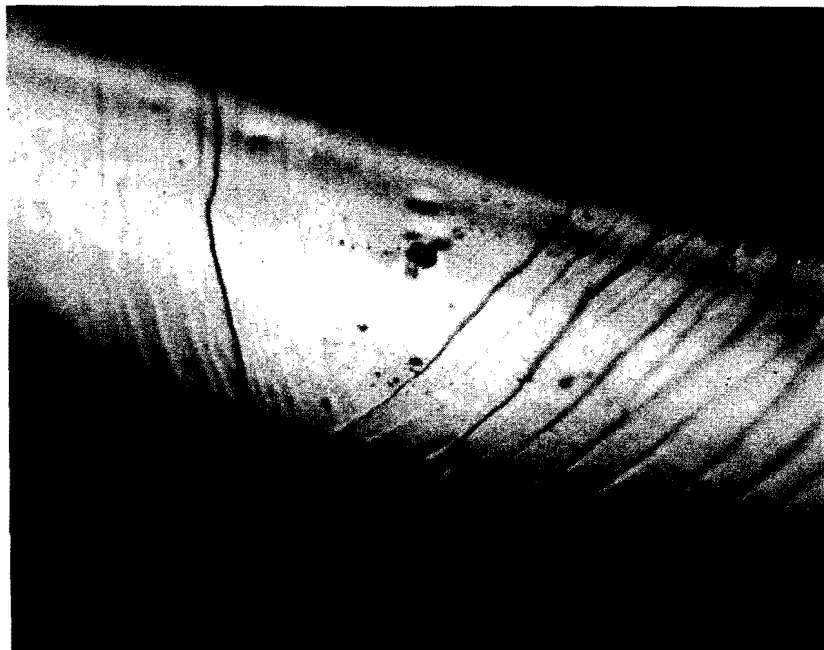
Figure 15. Cross-Slip in Platinum Where the Wire Has Started to Neck 375X
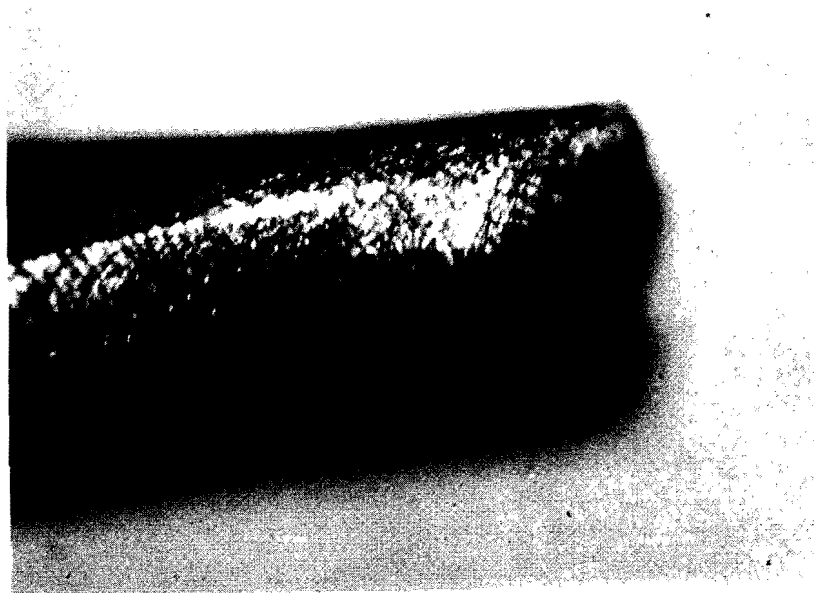
Figure 16. Configuration of Slip Lines in Platinum Within the Fracture Area 180X

Figure 17. Slip Lines in an Area Near the Fracture Area in Platinum 375X
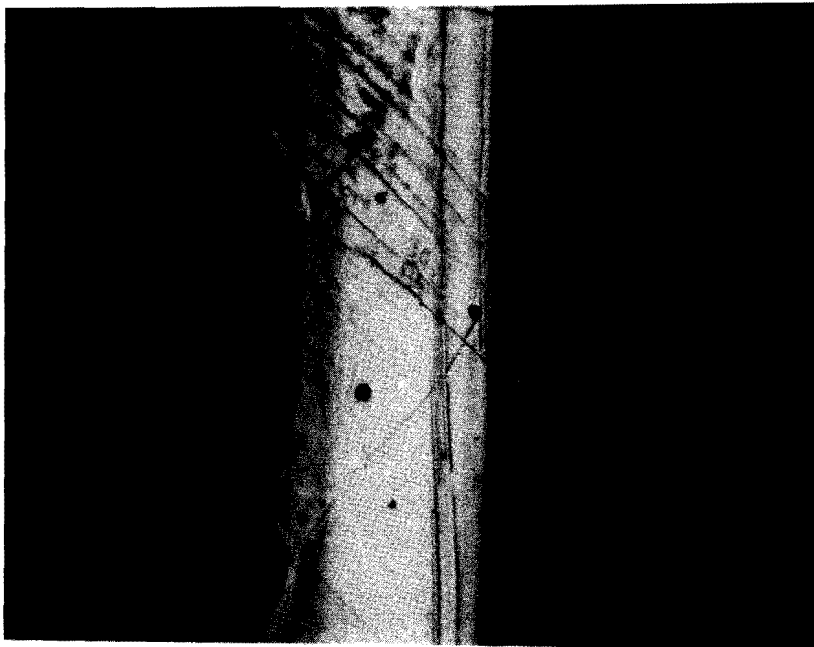
Figure 18. Nature of Slip Lines in Platinum as they Cross a Grain Boundary 375X
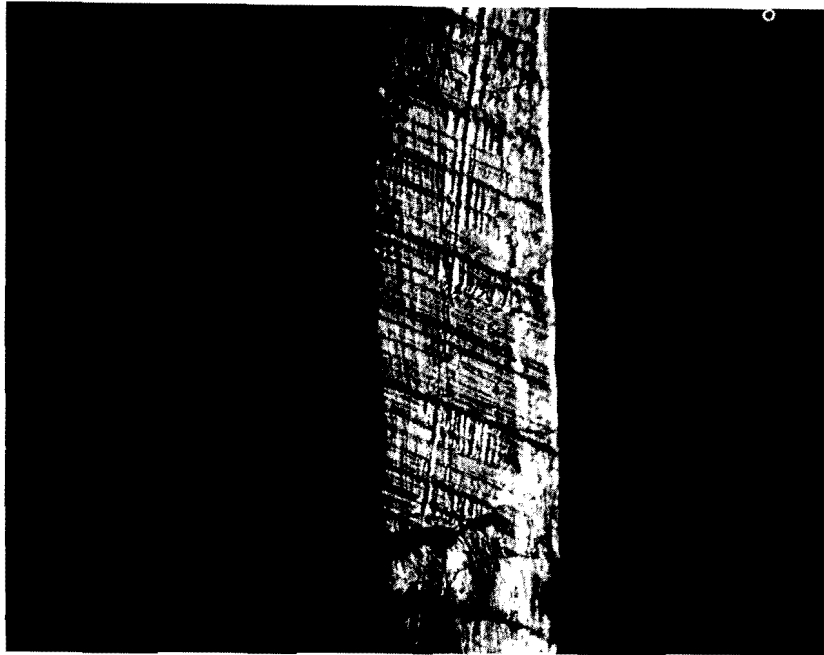
Figure 19. Parallel Slip Lines in Platinum 130X

Figure 20. Parallel Slip Lines in Platinum 375X
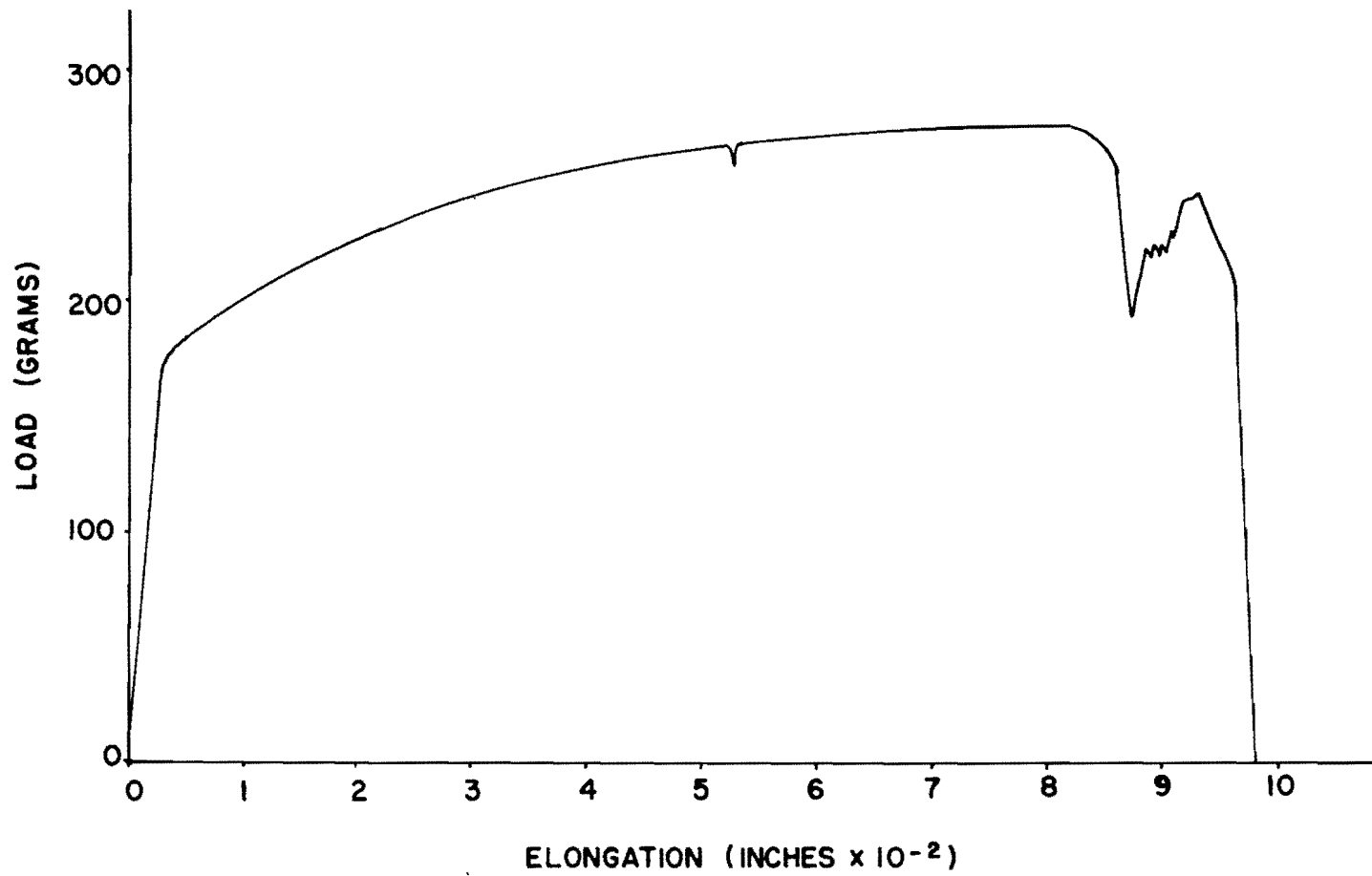
Figure 21. Typical Load-Elongation Curve for Platinum
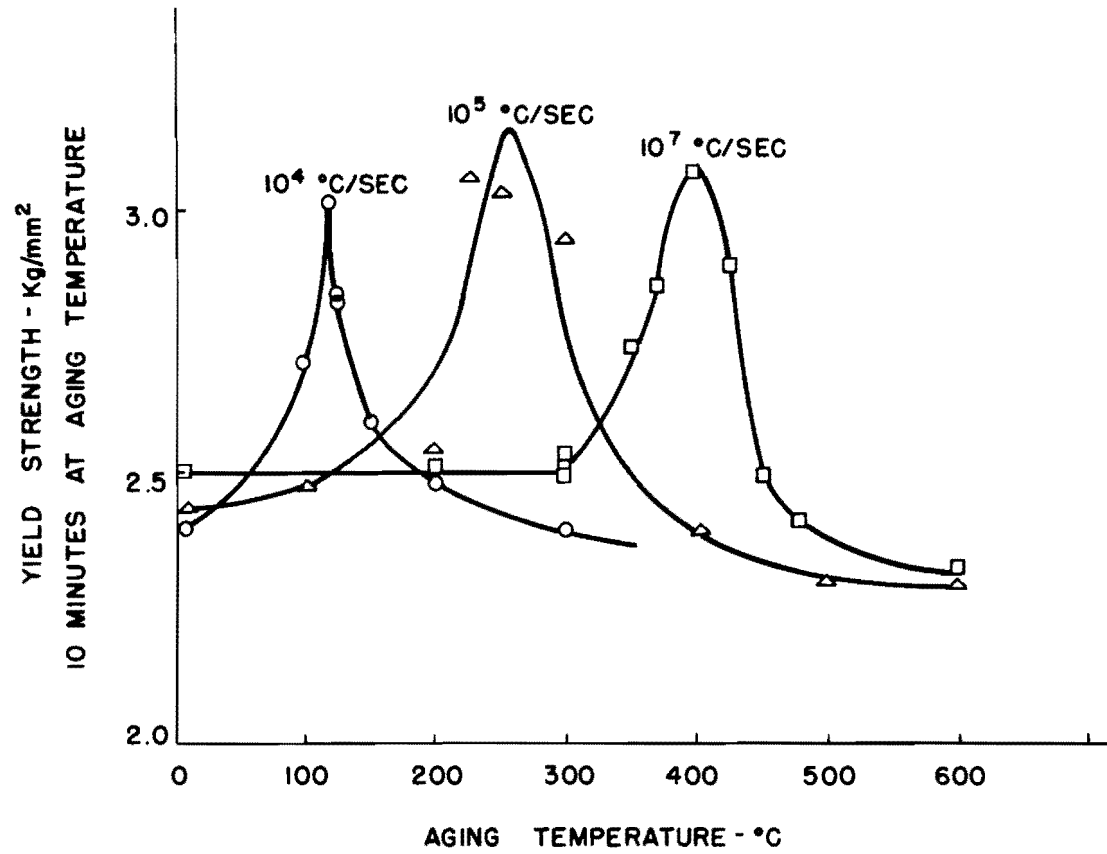
Figure 22. Influence of Quenching Rate on the Temperature Recovery Range for Gold

YIELD STRENGTH CHANGE At 100°C As A FUNCTION
Of AGING TIME For GOLD
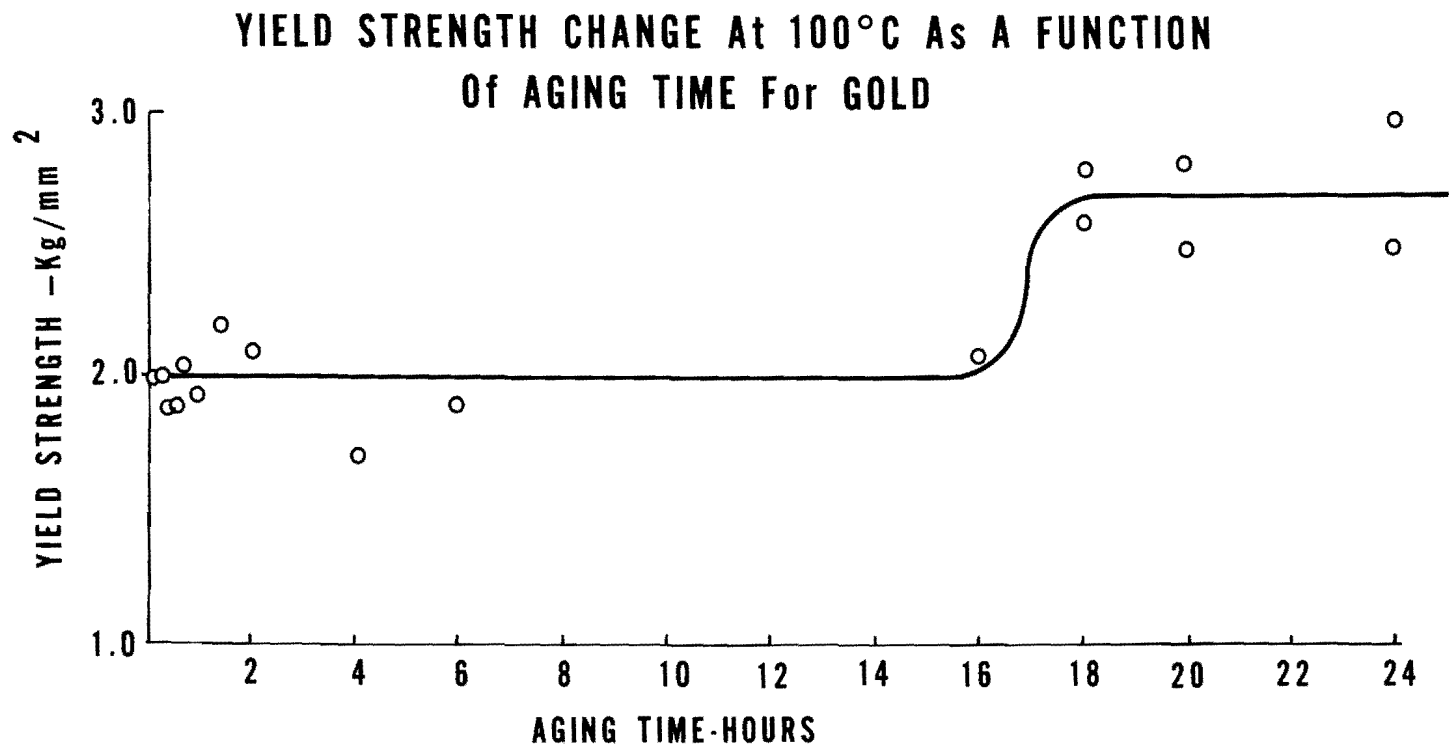
Figure 23.   Short Time Isothermal Aging Curve for Gold at 100°C
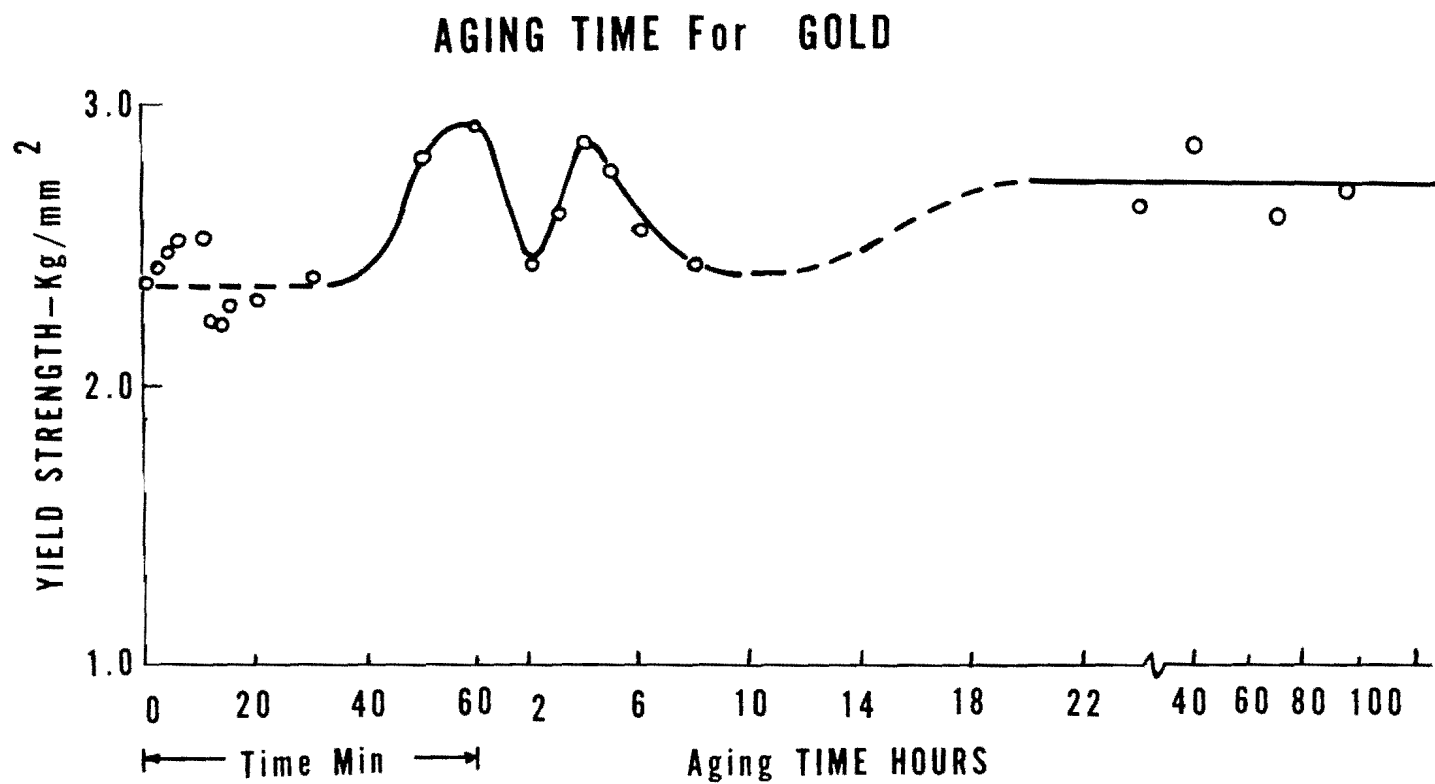
AGING TIME For GOLD

Figure 24. Short Time Isothermal Aging Curves for Gold at 200°C
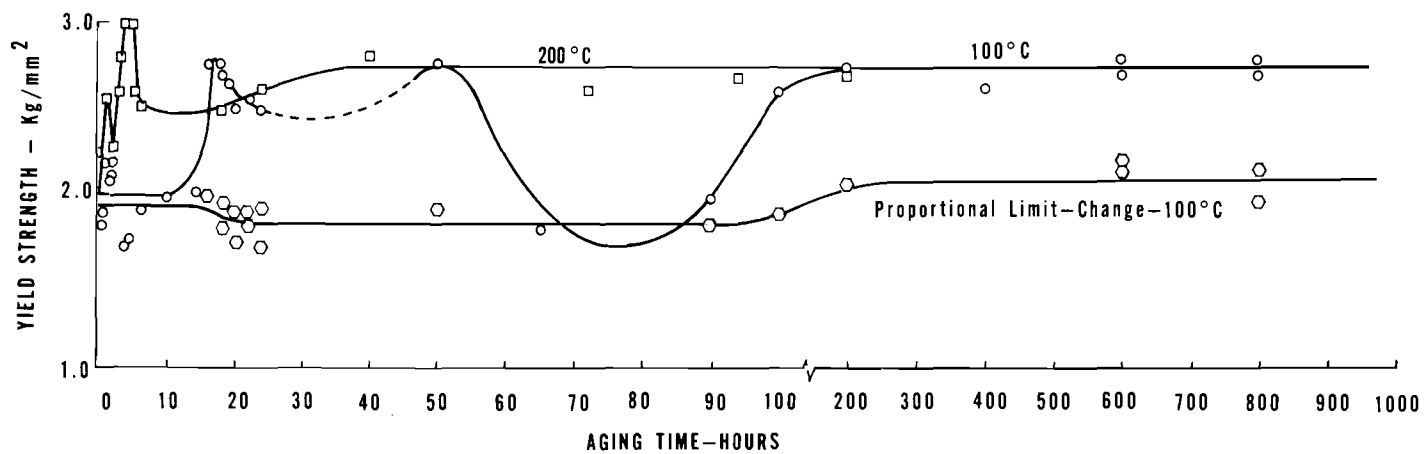
Figure 25. Isothermal Aging Curves for Gold at 100°C and 200°C with a Plot of a Change in the Proportional Limit
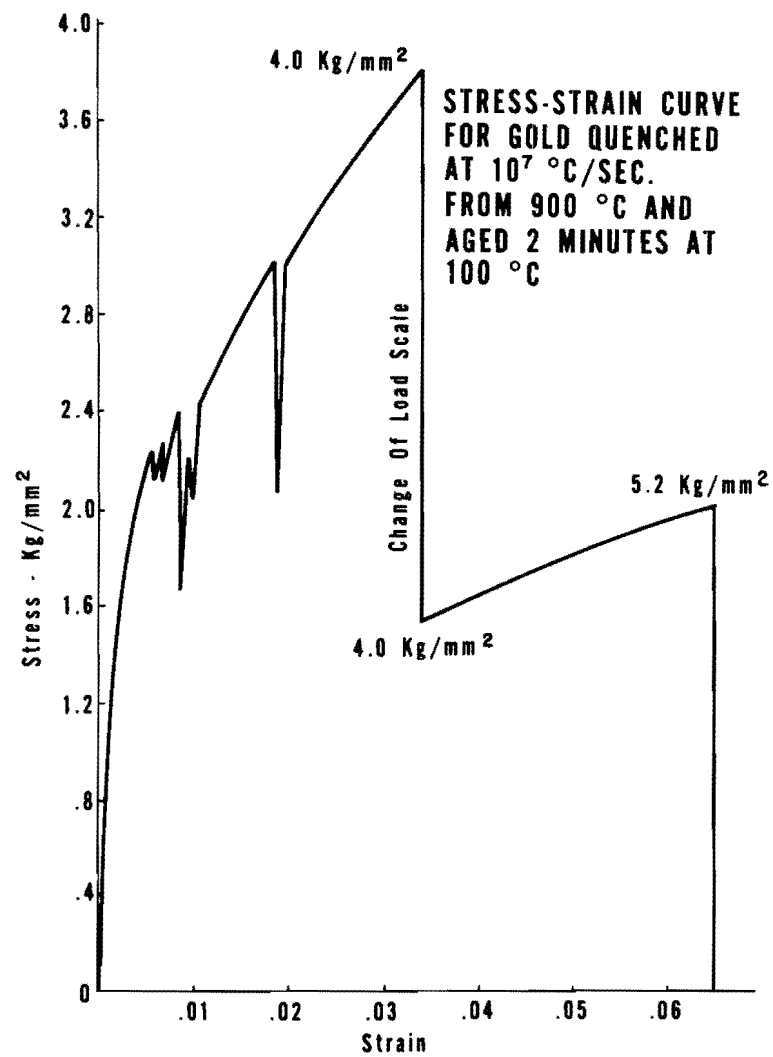
Figure 26. Serrated Stress-Strain Curve for Gold
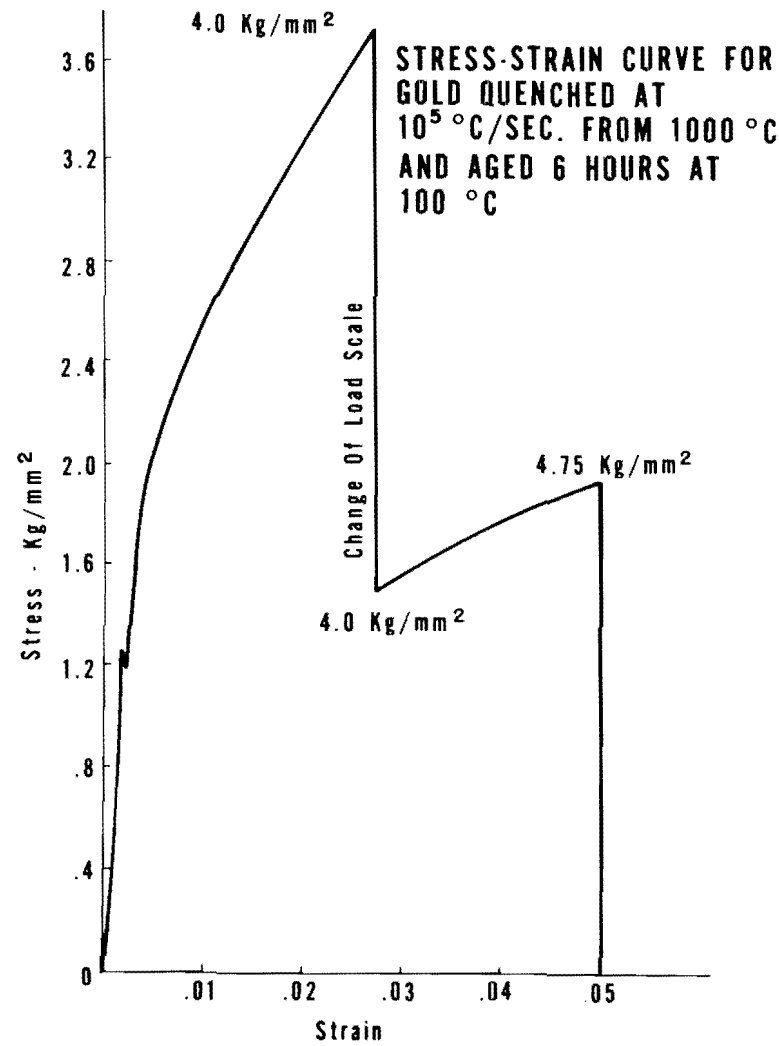
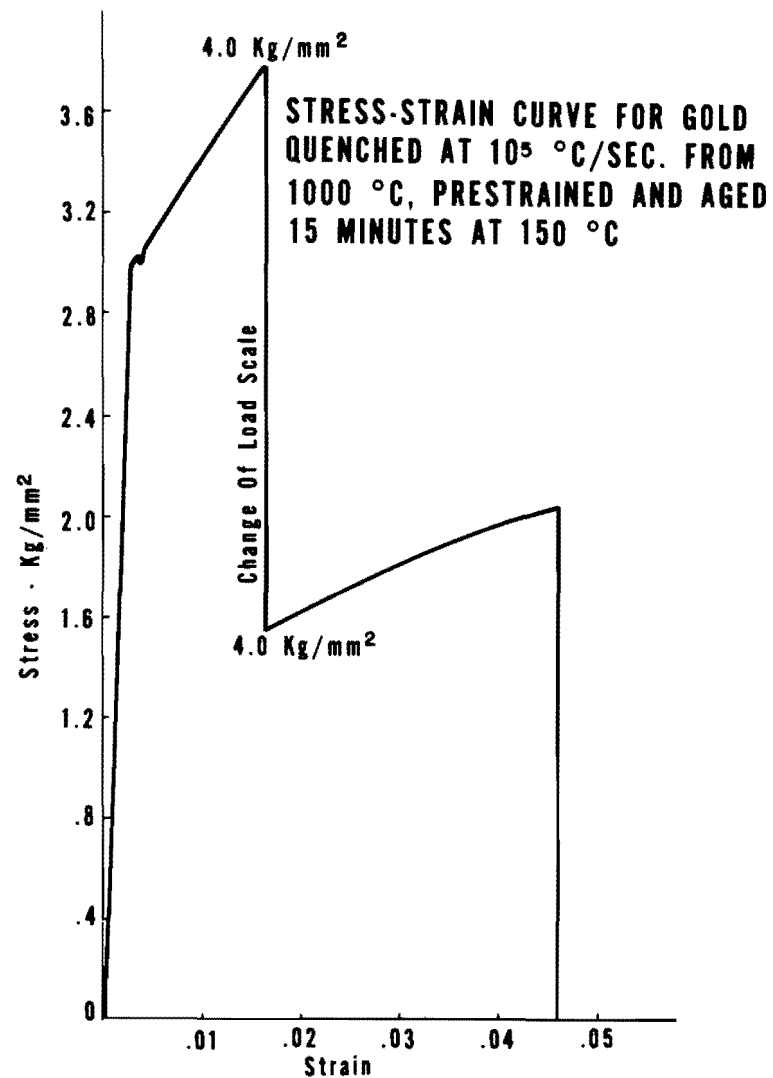Figure 27. A Small Yield Point in Stress-Strain Curve for Gold

Figure 28. Stress-Strain Curve for a Gold Wire Prestrained After Thermal
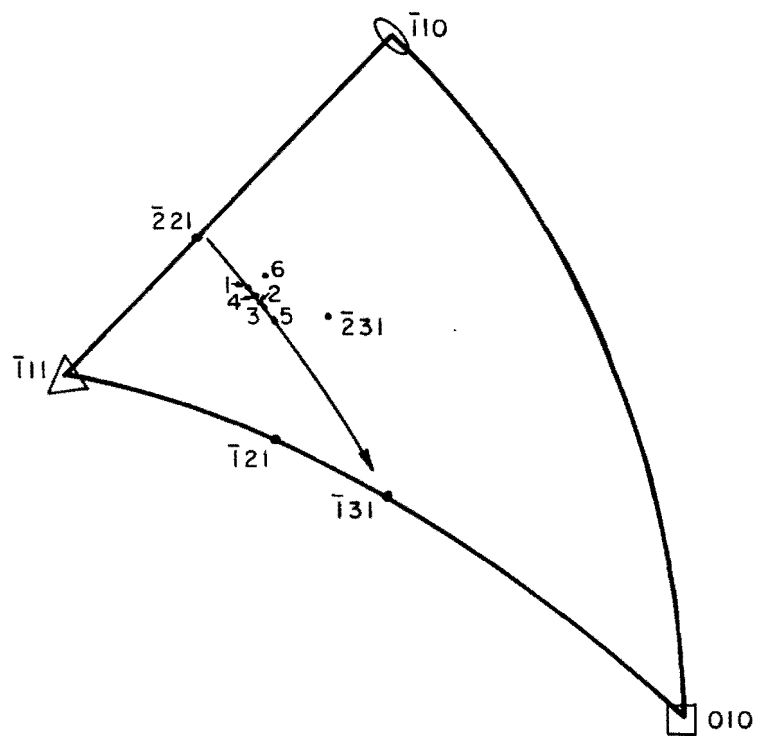Treatment Showing a Yield Point

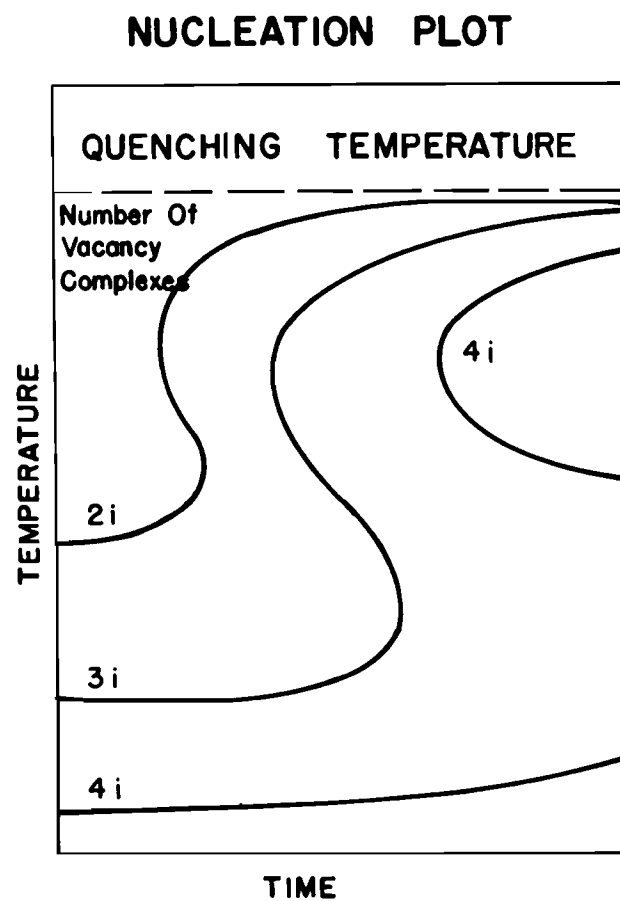Figure 29. Rotation of Gold Fiber Axis at Various Amounts of Plastic Strain

NUCLEATION PLOT

QUENCHING TEMPERATURE

Number Of
Vacancy
Complexes

4 i

2 i

3 i

4 i

TEMPERATURE

TIME

Figure 30. Generalized Time-Temperature-Nucleation Plot

ANNIHILATION PLOT

QUENCHING TEMPERATURE

Per Cent Annihilated
10

20

75
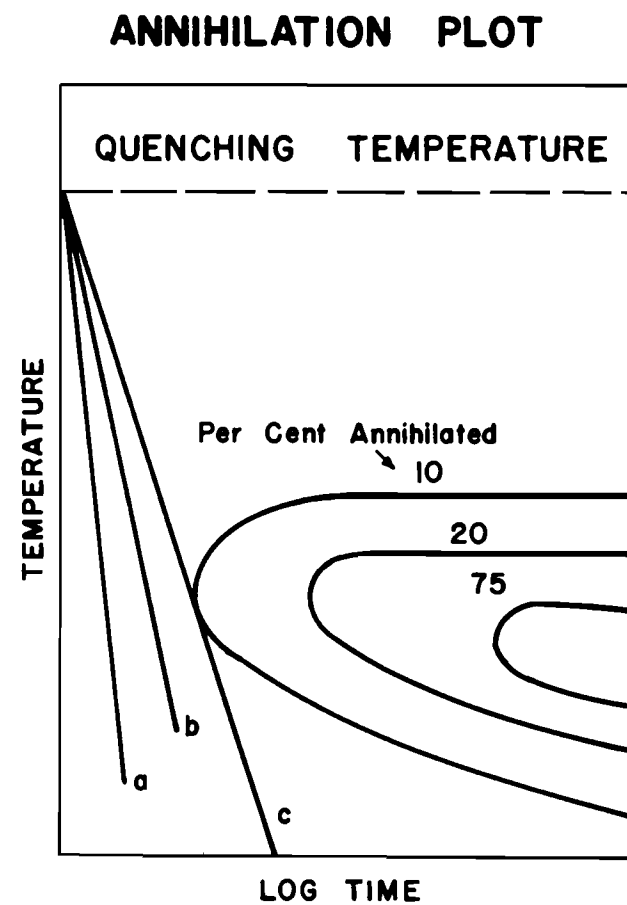
b

a

c

TEMPERATURE

LOG TIME

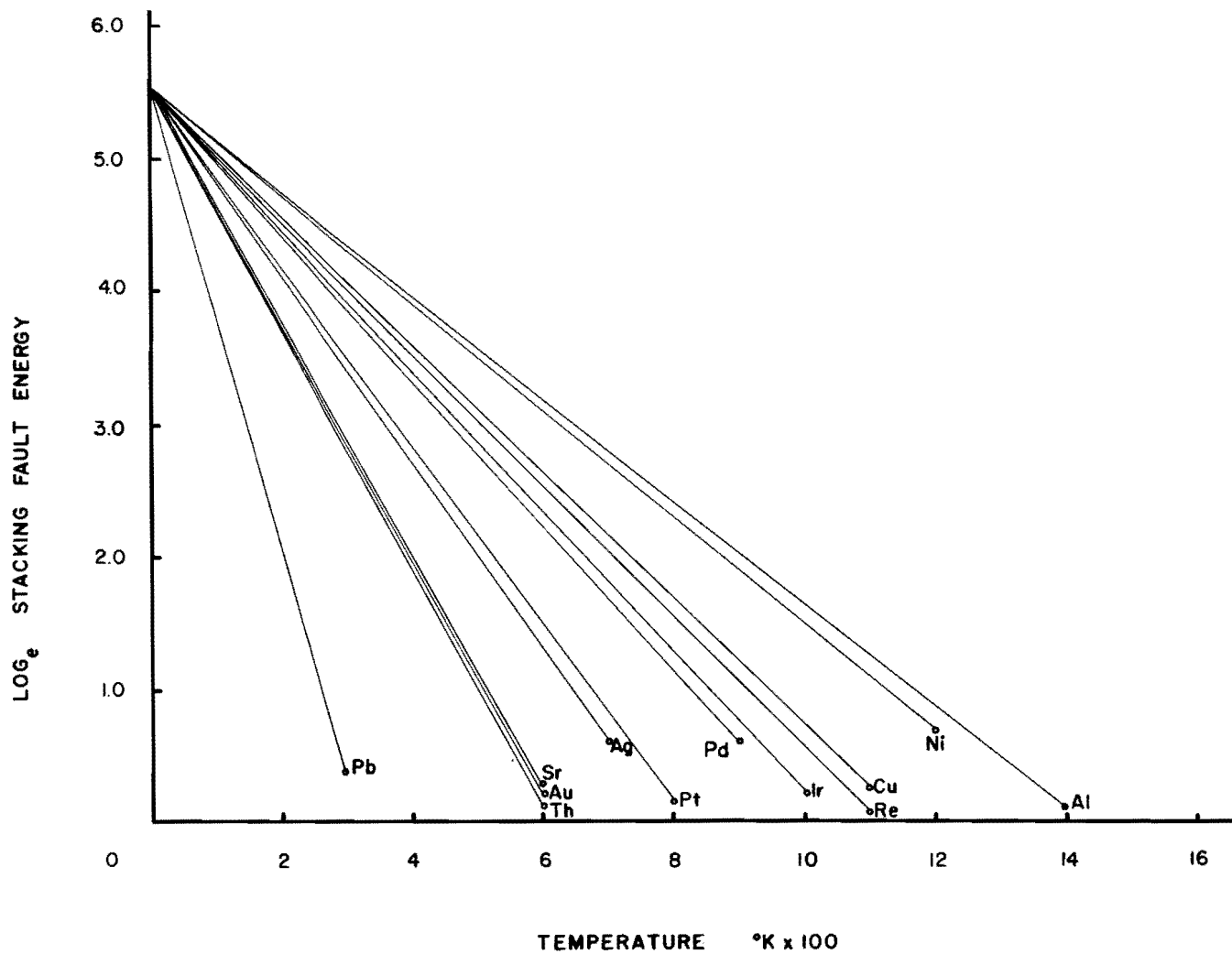Figure 31. Generalized Time-Temperature-Annihilation Plot

Figure 32. Stacking Fault Energies for F.C.C. Metals as a Function of Temperature